

Research Article

Molecular structural modeling and physical characteristics of anti-breast cancer drugs via some novel topological descriptors and regression models

Summeira Meharban^a, Asad Ullah^{a,*}, Shahid Zaman^b, Anila Hamraz^a, Abdul Razaq^c^a Department of Mathematical Sciences, Karakoram International University Gilgit, Gilgit, 15100, Pakistan^b Department of Mathematics, University of Stalkot, Stalkot, 51310, Pakistan^c Department of Biological Sciences, Karakoram International University Gilgit, Gilgit, 15100, Pakistan

ARTICLE INFO

Handling Editor: Dr A Wlodawer

Keywords:

Drugs
Molecular structure
Topological indices
Graph theory
QSPR analysis

ABSTRACT

Research is continuously being pursued to treat cancer patients and prevent the disease by developing new medicines. However, experimental drug design and development is a costly, time-consuming, and challenging process. Alternatively, computational and mathematical techniques play an important role in optimally achieving this goal. Among these mathematical techniques, topological indices (TIs) have many applications in the drugs used for the treatment of breast cancer. TIs can be utilized to forecast the effectiveness of drugs by providing molecular structure information and related properties of the drugs. In addition, these can assist in the design and discovery of new drugs by providing insights into the structure-property/structure-activity relationships. In this article, a Quantitative Structure Property Relationship (QSPR) analysis is carried out using some novel degree-based molecular descriptors and regression models to predict various properties (such as boiling point, melting point, enthalpy, flashpoint, molar refraction, molar volume, and polarizability) of 14 drugs used for the breast cancer treatment. The molecular structures of these drugs are topologically modeled through vertex and edge partitioning techniques of graph theory, and then linear regression models are developed to correlate the computed values with the experimental properties of the drugs to investigate the performance of TIs in predicting these properties. The results confirmed the potential of the considered topological indices as a tool for drug discovery and design in the field of breast cancer treatment.

1. Introduction

One of the major causes of death in the world is cancer. Cancer is a broad term used to describe a group of diseases characterized by the uncontrolled growth and spread of abnormal cells in the body. These cells can invade nearby tissues and organs, disrupting their normal function, and can also metastasize, spreading to other parts of the body through the bloodstream or lymphatic system. Breast cancer specifically refers to cancer that develops in the cells of the breast tissue. It is the most common cancer among women globally. Breast cancer can manifest in different forms, including invasive ductal carcinoma (which starts in the milk ducts and spreads to nearby tissues), invasive lobular carcinoma (which originates in the lobules or milk-producing glands), and less common subtypes such as inflammatory breast cancer and triple-negative breast cancer (Figuerola and Avila, 2019; Kinteh et al., 2023; Waks and Winer, 2019). Risk factors for breast cancer include age, family history of the disease, genetic mutations (such as BRCA1 and

BRCA2), hormonal factors (such as early menstruation, late menopause, and hormone replacement therapy), lifestyle factors (such as alcohol consumption, obesity, and physical inactivity), and exposure to ionizing radiation. Early detection through screening mammography, clinical breast exams, and breast self-exams, followed by prompt diagnosis and treatment, can significantly improve outcomes for individuals with breast cancer. Treatment options may include surgery, radiation therapy, chemotherapy, hormonal therapy, targeted therapy, or a combination of these approaches, depending on the type and stage of the cancer. (M. C. Shanmukha et al., 2022).

Over the past 20 years, research into breast cancer has significantly advanced our understanding of the condition and produced more effective, less harmful treatments. Early diagnosis at stages amenable to complete surgical resection and curative therapy has been made possible by increased public awareness and enhanced screening. As a result, survival rates for breast cancers have considerably increased, especially in younger women (Gao et al., 2016a). Major investment in breast

* Corresponding author.

E-mail address: dr.asadullah@kiu.edu.pk (A. Ullah).

cancer research and understanding has contributed to improvements in the detection and cure of breast cancer. Due in large part to variables like early discovery, frequent thorough screening, and a better knowledge of the disease, the breast cancer survival ratio has increased and the number of deaths related to this disease is constantly reducing (Kumar et al., 2015). Using preventive drugs or undergoing preventive surgery can lower the risk of breast cancer in people with a strong family background of the disease or who have been identified as having pre-cancerous breasts.

Research is continuously being pursued to treat cancer patients and prevent the disease by developing new medicines. However, experimental drug design and development is a costly, time-consuming, and challenging process. Alternatively, computational and mathematical techniques play an important role in achieving this goal in an optimal way. Among these computational and mathematical techniques, topological indices (TIs) have many applications in the drugs used for the treatment of breast cancer. The TI is the outcome of a logical and mathematical process that converts the chemical information provided within a graphical representation of a molecule into a helpful component or the outcome of certain standardized experiments (Arockiaraj et al., 2023; Liu et al., 2022; Paul et al., 2023; Ullah et al., 2023a,b; Asad Ullah, Muhammad Qasim et al., 2022; Ullah et al., 2023; Asad Ullah, Shamsudin et al., 2022; A. Ullah et al., 2022a,b,c). It is noted that the word "helpful" has particular implications. It means that the number can provide further explanations for how to interpret molecular properties and/or that it can contribute to a model for the prediction of a particular interesting attribute of molecules (Arockiaraj et al., 2019; Hayat et al., 2023; Hayat et al., 2022; Hayat et al., 2023a, 2023b; Yan et al., 2023; Zaman et al., 2023; Zaman et al., 2022). TIs can be utilized to forecast the effectiveness of drugs in cancer treatment by providing molecular structure information and related properties of the drugs (Bokhary et al., 2021; Gao et al., 2016b; M. Shanmukha et al., 2022). One can easily identify the most effective drugs for treatment through an in-depth investigation of degree-based TIs (M. Shanmukha et al., 2022). In addition, these can assist in the design and discovery of new drugs by providing insights into the structure-activity/structure-property relationships (Zhong et al., 2021).

In chemical graph theory, the molecular structure is modeled using a graph where vertices are atoms of the compound and edges are chemical bonds between atoms (Aslam et al., 2017b; Hakeem et al., 2023; Hosamani et al., 2017; Jahanbani et al., 2021; Siddiqui et al., 2022; Ullah et al., 2023; Yan et al., 2023; Yu et al., 2023; Zaman et al., 2023b; Zaman and Ullah, 2023; Zhang et al., 2023). A relatively new field called Cheminformatics combines mathematics, chemistry, and information science, it studies Quantitative structure property/activity relationship (QSPR/QSAR) that are used to calculate the biological activities and properties of different chemical compounds. TIs play an important role in QSPR/QSAR analysis in the fields of biological, chemical sciences, and engineering (Aslam et al., 2017b; Gutman et al., 2018). In QSAR modeling, the predictors consist of physico-chemical properties or theoretical molecular descriptors (Muhammad et al., 2018; Todeschini and Consonni, 2009; Xu et al., 2007), while the term QSPR models as response variable (Joudaki and Shafiei, 2020; Nantasenamat et al., 2009, 2010; Varmuza et al., 2013). Wiener (1947) gave the idea of a topological index during the investigation of the boiling point of paraffin and termed it a path number. After this, it was called as Wiener index. It is the first and most reputed topological index, both from an application as well as theoretical point of view, and is defined as the sum of the distance between all pairs of vertices in a graph G (Janoschek, 1987). Degree-based topological indices are commonly used and play a significant role in chemical graph theory, especially in chemistry. Gutman and Trinajstić established the earliest topological indices, the Zagreb type indices (Ali et al., 2020; Furtula et al., 2013; Gutman and Trinajstić, 1972; Kwun et al., 2018), which have been utilized to investigate molecular difficulty, boiling point, and chirality. Several researchers have investigated the QSPR and QSAR analysis of the molecular structures of

drugs by leveraging degree based topological indices (Bokhary et al., 2021; Mondal et al., 2021; Rauf et al., 2022; Ullah et al., 2024; Zhong et al., 2021) in order to gain a deeper understanding of their behavior and physical properties. However, despite intensive studies, the molecular structural topology is still not well understood. Here, in order to better understand the molecular structural topology and behavior of the drug molecules, we developed specific novel neighborhood degree based descriptors through mathematical expressions. These descriptors provide a more detailed understanding of the topology of drug molecules. The definitions and details of these descriptors are presented below.

In the present study, we have represented the molecular structure of drugs by a simple, finite, and connected graph $G(V, E)$ with $V(G)$, $E(G)$ defined as vertices and edges in G respectively (Randic, 1996). The distance of the shortest path between two vertices u and v in G is used to express the distance between them as $d(u, v) = d_G(u, v)$. The number of vertices of the graph adjacent to a given vertex v is the degree of that vertex and will be symbolized by η_G . Chemistry's valence concept and the concept of degree are closely related (Mc et al., 2020). To predict the physical characteristics of the drugs accurately, linear regression and QSPR modeling are used (Duchowicz et al., 2008; Hosamani et al., 2017).

The considered topological indices based on the vertex degree are as follows:

The modified neighborhood version of the forgotten topological index (Furtula and Gutman, 2015) is defined as,

$$F_N^*(G) = \sum_{uv \in E(G)} [\eta_G(u)^2 + \eta_G(v)^2]. \quad (1)$$

The neighborhood version of the second Zagreb index is describe by (Siddiqui et al., 2016)

$$M_2^*(G) = \sum_{uv \in E(G)} [\eta_G(u) \cdot \eta_G(v)]. \quad (2)$$

The neighborhood version of the hyper Zagreb index is described as (Shirdel et al., 2013)

$$HM_N(G) = \sum_{uv \in E(G)} [\eta_G(u) + \eta_G(v)]^2. \quad (3)$$

The neighborhood Zagreb index is defined as,

$$M_N(G) = \sum_{v \in V(G)} [\eta_G(v)]^2. \quad (4)$$

The neighborhood version of the forgotten topological index, which is defined as,

$$F_N(G) = \sum_{v \in V(G)} [\eta_G(v)]^3. \quad (5)$$

for further details about the above indices, see (Mondal et al., 2019).

2. Results and discussion

2.1. Computation of topological indices

The chemical structures of drugs used to treat breast cancer are subjected to some novel degree-based topological indices (Eqs. (1)–(5)). It is already established that the degree based topological indices are closely linked to the physical characteristics of the chemical compounds (Aslam et al., 2017; Mondal et al., 2019; Shao et al., 2018; Siddiqui et al., 2016). Here, we have represented the molecular structure of drugs by a simple, finite, and connected graph $G(V, E)$ with $V(G)$, $E(G)$ defined as vertices and edges in G respectively (Randic, 1996). The number of vertices of the graph adjacent to a given vertex v is the degree of that

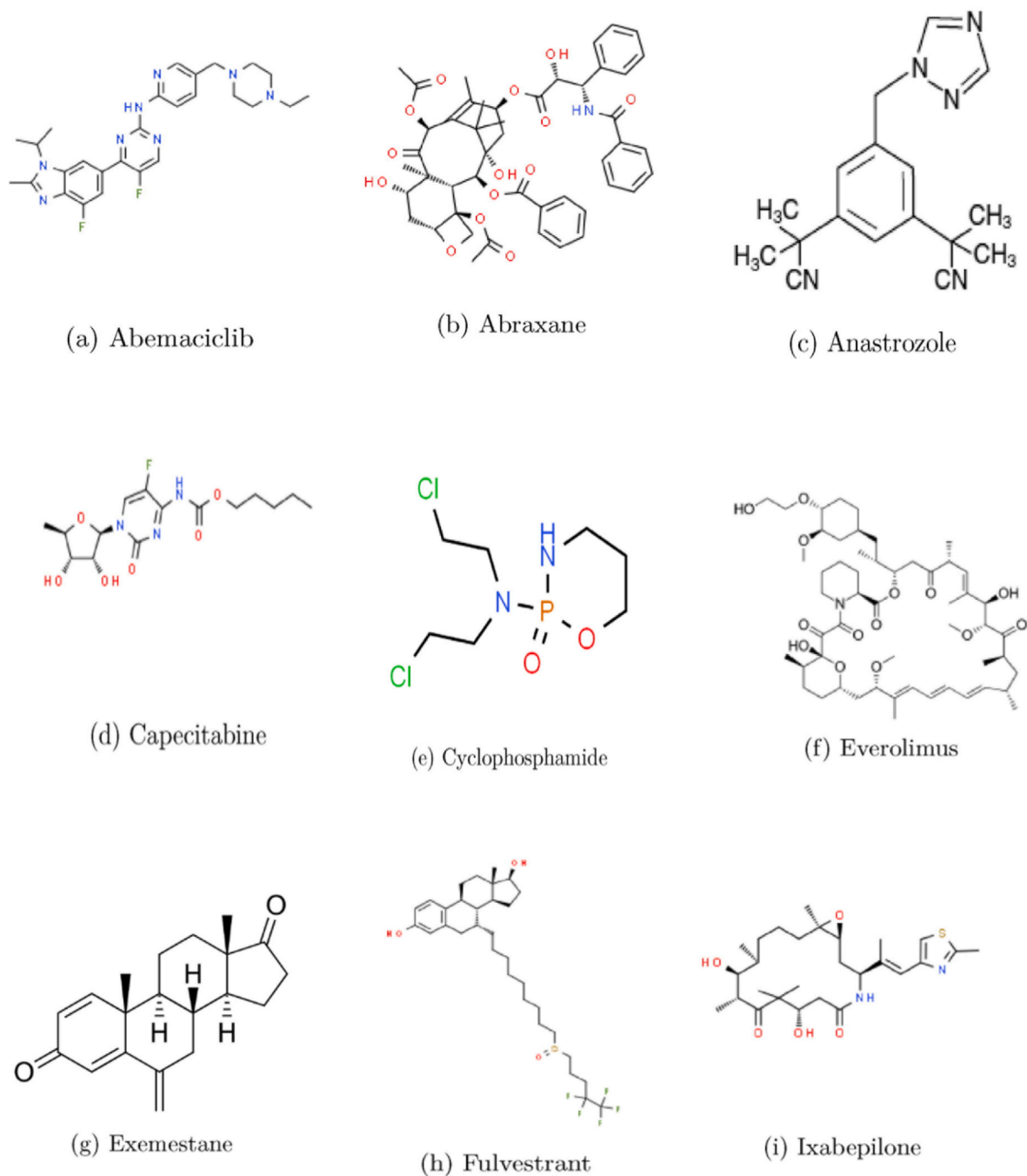


Fig. 1. Molecular structures of anti-breast cancer drugs.

vertex and will be symbolized by η_G and the term frequency is defined here as, the division of edge(vertex) set into partitions according to their sum of neighborhood degree. In this section, the molecular structures of 14 drugs [Abemaciclib (Verzenio), braxane, Anastrozole (Arimidex), Capecitabine (Xeloda), Cyclophosphamide, Everolimus (Afinitor), Exemestane (Aromasin), Fulvestrant (Faslodex), Ixabepilone (Ixemptra), Letrozole (Femara), Megestrol Acetate, Methotrexate, Tamoxifen (Soltamox), and Thiotepa (Tepadina)] are taken to compute some novel topological indices. Fig. 1 shows the molecular structures of these medications. The constituents in the chemical structure are thought of as nodes/vertices of the graph, and the connections between them are as edges. Graph theory-based edge and vertex partitioning techniques are then used to model the molecular topology and to compute the

frequency of edges and vertices, these frequencies are given in the form of tables in the relevant sections below. The topological indices are computed based on these frequency tables and Eqs. (1)–(5).

Theorem 1. Let G_1 be the graph of abemaciclib, then the topological indices (Eqs. (1)–(5)) for G_1 are given as follows:

1. $F_N^*(G_1) = 8018$
2. $M_2^*(G_1) = 3613$
3. $HM_N(G_1) = 15242$
4. $M_N(G_1) = 2776$
5. $F_N(G_1) = 21806$

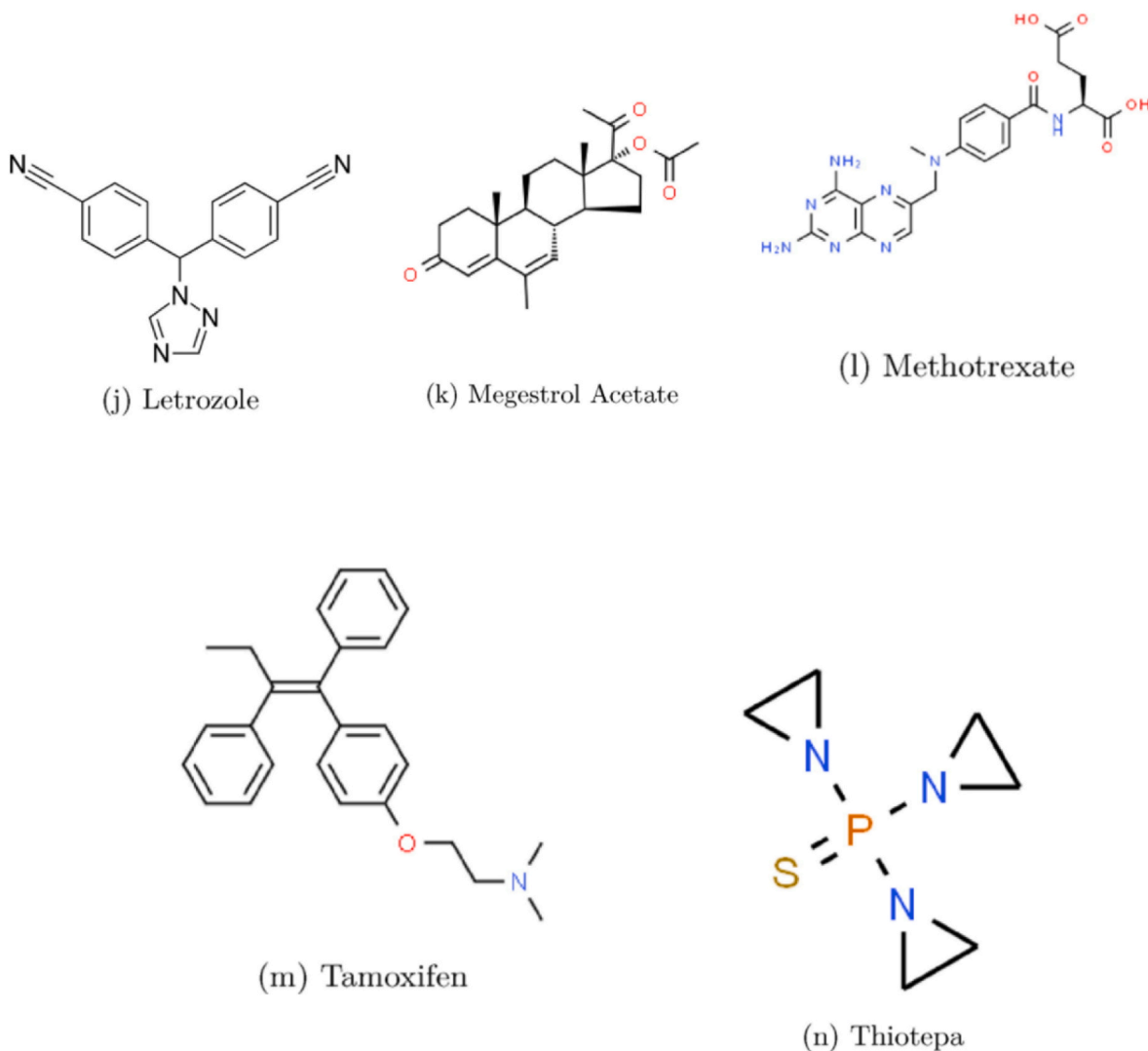


Fig. 1. (continued).

Proof. Let G_1 be the graph of Abemaciclib with vertex set V and edge set E . Let $\eta_v(G)$ represent degree of a vertex and $E_{s,t}$ represents the class of edges of G_1 joining vertices of degrees s and t . Here, the edge(vertex) set is divided into partitions according to their sum of neighborhood degree, called the frequency, which is shown in below tables. [Tables i and ii](#) show the vertex partition and edge partition respectively.

Table i
Vertex partition of Abemaciclib drug.

$\eta_v(G)$	Frequency
3	9
4	25
6	7
7	12
8	4
9	7
10	2
12	3

$$\begin{aligned}
 &= \sum_{uv \in E_1} [\eta_G(u)^2 + \eta_G(v)^2] + \sum_{uv \in E_2} [\eta_G(u)^2 + \eta_G(v)^2] + \sum_{uv \in E_3} [\eta_G(u)^2 \\
 &+ \eta_G(v)^2] + \sum_{uv \in E_4} [\eta_G(u)^2 + \eta_G(v)^2] + \sum_{uv \in E_5} [\eta_G(u)^2 + \eta_G(v)^2] \\
 &+ \sum_{uv \in E_6} [\eta_G(u)^2 + \eta_G(v)^2] + \sum_{uv \in E_7} [\eta_G(u)^2 + \eta_G(v)^2] + \sum_{uv \in E_8} [\eta_G(u)^2 \\
 &+ \eta_G(v)^2] + \sum_{uv \in E_9} [\eta_G(u)^2 + \eta_G(v)^2] + \sum_{uv \in E_{10}} [\eta_G(u)^2 + \eta_G(v)^2] \\
 &+ \sum_{uv \in E_{11}} [\eta_G(u)^2 + \eta_G(v)^2] + \sum_{uv \in E_{12}} [\eta_G(u)^2 + \eta_G(v)^2] + \sum_{uv \in E_{13}} [\eta_G(u)^2 \\
 &+ \eta_G(v)^2] + \sum_{uv \in E_{14}} [\eta_G(u)^2 + \eta_G(v)^2] + \sum_{uv \in E_{15}} [\eta_G(u)^2 + \eta_G(v)^2] \\
 &+ \sum_{uv \in E_{16}} [\eta_G(u)^2 + \eta_G(v)^2] + \sum_{uv \in E_{17}} [\eta_G(u)^2 + \eta_G(v)^2] + \sum_{uv \in E_{18}} [\eta_G(u)^2 \\
 &+ \eta_G(v)^2] + \sum_{uv \in E_{19}} [\eta_G(u)^2 + \eta_G(v)^2] + \sum_{uv \in E_{20}} [\eta_G(u)^2 + \eta_G(v)^2] \\
 &+ \sum_{uv \in E_{21}} [\eta_G(u)^2 + \eta_G(v)^2] + \sum_{uv \in E_{22}} [\eta_G(u)^2 + \eta_G(v)^2] + \sum_{uv \in E_{23}} [\eta_G(u)^2 \\
 &+ \eta_G(v)^2] + \sum_{uv \in E_{24}} [\eta_G(u)^2 + \eta_G(v)^2]
 \end{aligned}$$

1. By using Eq. (1) and edge partitions given in [Table ii](#) we get,

$$F_N^*(G) = \sum_{uv \in E(G)} [\eta_G(u)^2 + \eta_G(v)^2].$$

$$\begin{aligned}
 &= [(3)^2 + (6)^2](1) + [(3)^2 + (7)^2](8) + [(4)^2 + (6)^2](3) + [(4)^2 \\
 &\quad + (7)^2](9) + [(4)^2 + (8)^2](2) + [(4)^2 + (9)^2](10) + [(4)^2 + (12)^2](1) \\
 &\quad + [(6)^2 + (6)^2](1) + [(6)^2 + (7)^2](4) + [(6)^2 + (8)^2](4) + [(6)^2 \\
 &\quad + (9)^2](2) + [(6)^2 + (10)^2](2) + [(7)^2 + (7)^2](4) + [(7)^2 + (8)^2](4) \\
 &\quad + [(7)^2 + (9)^2](3) + [(7)^2 + (10)^2](1) + [(7)^2 + (12)^2](1) + [(8)^2 \\
 &\quad + (9)^2](1) + [(8)^2 + (10)^2](1) + [(8)^2 + (12)^2](1) + [(9)^2 + (9)^2](2) \\
 &\quad + [(9)^2 + (10)^2](1) + [(9)^2 + (12)^2](5) + [(10)^2 + (12)^2](1) \\
 &= 8018
 \end{aligned}$$

2. By using Eq. (2) and edge partitions given in table ii we get,

$$\begin{aligned}
 M_2^*(G) &= \sum_{uv \in E(G)} [\eta_G(u) \cdot \eta_G(v)]. \\
 &= \sum_{uv \in E_1} [\eta_G(u) \cdot \eta_G(v)] + \sum_{uv \in E_2} [\eta_G(u) \cdot \eta_G(v)] + \sum_{uv \in E_3} [\eta_G(u) \cdot \eta_G(v)] \\
 &\quad + \sum_{uv \in E_4} [\eta_G(u) \cdot \eta_G(v)] + \sum_{uv \in E_5} [\eta_G(u) \cdot \eta_G(v)] + \sum_{uv \in E_6} [\eta_G(u) \cdot \eta_G(v)] \\
 &\quad + \sum_{uv \in E_7} [\eta_G(u) \cdot \eta_G(v)] + \sum_{uv \in E_8} [\eta_G(u) \cdot \eta_G(v)] + \sum_{uv \in E_9} [\eta_G(u) \cdot \eta_G(v)] \\
 &\quad + \sum_{uv \in E_{10}} [\eta_G(u) \cdot \eta_G(v)] + \sum_{uv \in E_{11}} [\eta_G(u) \cdot \eta_G(v)] + \sum_{uv \in E_{12}} [\eta_G(u) \cdot \eta_G(v)] \\
 &\quad + \sum_{uv \in E_{13}} [\eta_G(u) \cdot \eta_G(v)] + \sum_{uv \in E_{14}} [\eta_G(u) \cdot \eta_G(v)] + \sum_{uv \in E_{15}} [\eta_G(u) \cdot \eta_G(v)] \\
 &\quad + \sum_{uv \in E_{16}} [\eta_G(u) \cdot \eta_G(v)] + \sum_{uv \in E_{17}} [\eta_G(u) \cdot \eta_G(v)] + \sum_{uv \in E_{18}} [\eta_G(u) \cdot \eta_G(v)] \\
 &\quad + \sum_{uv \in E_{19}} [\eta_G(u) \cdot \eta_G(v)] + \sum_{uv \in E_{20}} [\eta_G(u) \cdot \eta_G(v)] + \sum_{uv \in E_{21}} [\eta_G(u) \cdot \eta_G(v)] \\
 &\quad + \sum_{uv \in E_{22}} [\eta_G(u) \cdot \eta_G(v)] + \sum_{uv \in E_{23}} [\eta_G(u) \cdot \eta_G(v)] + \sum_{uv \in E_{24}} [\eta_G(u) \cdot \eta_G(v)] \\
 &= [(3).(6)](1) + [(3).(7)](8) + [(4).(6)](3) + [(4).(7)](9) + [(4).(8)](2) \\
 &\quad + [(4).(9)](10) + [(4).(12)](1) + [(6).(6)](1) + [(6).(7)](4) \\
 &\quad + [(6).(8)](4) + [(6).(9)](2) + [(6).(10)](2) + [(7).(7)](4) \\
 &\quad + [(7).(8)](4) + [(7).(9)](3) + [(7).(10)](1) + [(7).(12)](2) \\
 &\quad + [(8).(9)](1) + [(8).(10)](1) + [(8).(12)](1) + [(9).(9)](2) \\
 &\quad + [(9).(10)](1) + [(9).(12)](5) + [(10).(12)](1) \\
 &= 3613
 \end{aligned}$$

3. By using Eq. (3) and the edge partitions given in Table ii we get

$$HM_N(G) = \sum_{uv \in E(G)} \left[\eta_G(u) + \eta_G(v) \right]^2.$$

$$\begin{aligned}
 &= \sum_{uv \in E_1} \left[\eta_G(u) + \eta_G(v) \right]^2 + \sum_{uv \in E_2} \left[\eta_G(u) + \eta_G(v) \right]^2 + \sum_{uv \in E_3} \left[\eta_G(u) + \eta_G(v) \right]^2 + \sum_{uv \in E_4} \left[\eta_G(u) + \eta_G(v) \right]^2 + \sum_{uv \in E_5} \left[\eta_G(u) + \eta_G(v) \right]^2 + \sum_{uv \in E_6} \left[\eta_G(u) + \eta_G(v) \right]^2 \\
 &\quad + \sum_{uv \in E_7} \left[\eta_G(u) + \eta_G(v) \right]^2 + \sum_{uv \in E_8} \left[\eta_G(u) + \eta_G(v) \right]^2 + \sum_{uv \in E_9} \left[\eta_G(u) + \eta_G(v) \right]^2 + \sum_{uv \in E_{10}} \left[\eta_G(u) + \eta_G(v) \right]^2 + \sum_{uv \in E_{11}} \left[\eta_G(u) + \eta_G(v) \right]^2 + \sum_{uv \in E_{12}} \left[\eta_G(u) \right. \\
 &\quad \left. + \eta_G(v) \right]^2 + \sum_{uv \in E_{13}} \left[\eta_G(u) + \eta_G(v) \right]^2 + \sum_{uv \in E_{14}} \left[\eta_G(u) + \eta_G(v) \right]^2 + \sum_{uv \in E_{15}} \left[\eta_G(u) + \eta_G(v) \right]^2 + \sum_{uv \in E_{16}} \left[\eta_G(u) + \eta_G(v) \right]^2 + \sum_{uv \in E_{17}} \left[\eta_G(u) \right. \\
 &\quad \left. + \eta_G(v) \right]^2 + \sum_{uv \in E_{18}} \left[\eta_G(u) + \eta_G(v) \right]^2 + \sum_{uv \in E_{19}} \left[\eta_G(u) + \eta_G(v) \right]^2 + \sum_{uv \in E_{20}} \left[\eta_G(u) + \eta_G(v) \right]^2 + \sum_{uv \in E_{21}} \left[\eta_G(u) + \eta_G(v) \right]^2 \\
 &\quad + \sum_{uv \in E_{22}} \left[\eta_G(u) + \eta_G(v) \right]^2 + \sum_{uv \in E_{23}} \left[\eta_G(u) + \eta_G(v) \right]^2 + \sum_{uv \in E_{24}} \left[\eta_G(u) + \eta_G(v) \right]^2
 \end{aligned}$$

$$\begin{aligned}
 &= [(3 + 6)^2](1) + [(3 + 7)^2](8) + [(4 + 6)^2](3) + [(4 + 7)^2](9) \\
 &\quad + [(4 + 8)^2](2) + [(4 + 9)^2](10) + [(4 + 12)^2](1) + [(6 + 6)^2](1) \\
 &\quad + [(6 + 7)^2](4) + [(6 + 8)^2](4) + [(6 + 9)^2](2) + [(6 + 10)^2](2) \\
 &\quad + [(7 + 7)^2](4) + [(7 + 8)^2](4) + [(7 + 9)^2](3) + [(7 + 10)^2](1) \\
 &\quad + [(7 + 12)^2](2) + [(8 + 9)^2](1) + [(8 + 10)^2](1) + [(8 + 12)^2](1) \\
 &\quad + [(9 + 9)^2](2) + [(9 + 10)^2](1) + [(9 + 12)^2](5) + [(10 + 12)^2](1) \\
 &= 15244
 \end{aligned}$$

4. By using Eq. (4) and vertex partitions given in Table i we get

$$\begin{aligned}
 M_N(G) &= \sum_{v \in V(G)} \left[\eta_G(v) \right]^2. \\
 &= \sum_{v \in V_1} \left[\eta_G(v) \right]^2 + \sum_{v \in V_2} \left[\eta_G(v) \right]^2 + \sum_{v \in V_3} \left[\eta_G(v) \right]^2 + \sum_{v \in V_4} \left[\eta_G(v) \right]^2 \\
 &\quad + \sum_{v \in V_5} \left[\eta_G(v) \right]^2 + \sum_{v \in V_6} \left[\eta_G(v) \right]^2 + \sum_{v \in V_7} \left[\eta_G(v) \right]^2 + \sum_{v \in V_8} \left[\eta_G(v) \right]^2 \\
 &= [(3)^2](9) + [(4)^2](25) + [(6)^2](7) + [(7)^2](12) + [(8)^2](4) \\
 &\quad + [(9)^2](7) + [(10)^2](2) + [(12)^2] \\
 &= 2776
 \end{aligned}$$

5. By using Eq. (5) and vertex partitions given in Table i we get

$$\begin{aligned}
 F_N(G) &= \sum_{v \in V(G)} \left[\eta_G(v) \right]^3. \\
 &= \sum_{v \in V_1} \left[\eta_G(v) \right]^3 + \sum_{v \in V_2} \left[\eta_G(v) \right]^3 + \sum_{v \in V_3} \left[\eta_G(v) \right]^3 + \sum_{v \in V_4} \left[\eta_G(v) \right]^3 + \sum_{v \in V_5} \left[\eta_G(v) \right]^3 \\
 &\quad + \sum_{v \in V_6} \left[\eta_G(v) \right]^3 + \sum_{v \in V_7} \left[\eta_G(v) \right]^3 + \sum_{v \in V_8} \left[\eta_G(v) \right]^3 \\
 &= [(3)^3](9) + [(4)^3](25) + [(6)^3](7) + [(7)^3](12) + [(8)^3](4) + [(9)^3](7) \\
 &\quad + [(10)^3](2) + [(12)^3](3) \\
 &= 21806
 \end{aligned}$$

Theorem 2. Let G_2 be the graph of Abraxane, and then the topological indices (Eqs. (1)–(5)) for G_2 are given as follows:

1. $F_N^*(G_2) = 14744$
2. $M_2^*(G_2) = 6504$
3. $HM_N(G_2) = 27752$
4. $M_N(G_2) = 4996$
5. $F_N(G_2) = 45064$

E' . Let $\eta'_v(G)$ represent the degree of a vertex and represent the class of edges of G_2 joining vertices of degrees s and t . The following tables show the vertex partition and edge partition.

1. By using Eq. (1) and edge partitions given in Table iv we get,

$$F_N^*(G) = \sum_{uv \in E(G)} [\eta_G(u)^2 + \eta_G(v)^2].$$

$$\begin{aligned} &= \sum_{uv \in E_1} [\eta_G(u)^2 + \eta_G(v)^2] + \sum_{uv \in E_2} [\eta_G(u)^2 + \eta_G(v)^2] + \sum_{uv \in E_3} [\eta_G(u)^2 + \eta_G(v)^2] + \sum_{uv \in E_4} [\eta_G(u)^2 + \eta_G(v)^2] + \sum_{uv \in E_5} [\eta_G(u)^2 + \eta_G(v)^2] + \sum_{uv \in E_6} [\eta_G(u)^2 + \eta_G(v)^2] \\ &+ \sum_{uv \in E_7} [\eta_G(u)^2 + \eta_G(v)^2] + \sum_{uv \in E_8} [\eta_G(u)^2 + \eta_G(v)^2] + \sum_{uv \in E_9} [\eta_G(u)^2 + \eta_G(v)^2] + \sum_{uv \in E_{10}} [\eta_G(u)^2 + \eta_G(v)^2] + \sum_{uv \in E_{11}} [\eta_G(u)^2 + \eta_G(v)^2] \\ &+ \sum_{uv \in E_{12}} [\eta_G(u)^2 + \eta_G(v)^2] + \sum_{uv \in E_{13}} [\eta_G(u)^2 + \eta_G(v)^2] + \sum_{uv \in E_{14}} [\eta_G(u)^2 + \eta_G(v)^2] + \sum_{uv \in E_{15}} [\eta_G(u)^2 + \eta_G(v)^2] + \sum_{uv \in E_{16}} [\eta_G(u)^2 + \eta_G(v)^2] \\ &+ \sum_{uv \in E_{17}} [\eta_G(u)^2 + \eta_G(v)^2] + \sum_{uv \in E_{18}} [\eta_G(u)^2 + \eta_G(v)^2] + \sum_{uv \in E_{19}} [\eta_G(u)^2 + \eta_G(v)^2] + \sum_{uv \in E_{20}} [\eta_G(u)^2 + \eta_G(v)^2] + \sum_{uv \in E_{21}} [\eta_G(u)^2 + \eta_G(v)^2] \\ &+ \sum_{uv \in E_{22}} [\eta_G(u)^2 + \eta_G(v)^2] + \sum_{uv \in E_{23}} [\eta_G(u)^2 + \eta_G(v)^2] + \sum_{uv \in E_{24}} [\eta_G(u)^2 + \eta_G(v)^2] + \sum_{uv \in E_{25}} [\eta_G(u)^2 + \eta_G(v)^2] + \sum_{uv \in E_{26}} [\eta_G(u)^2 + \eta_G(v)^2] \\ &+ \sum_{uv \in E_{27}} [\eta_G(u)^2 + \eta_G(v)^2] + \sum_{uv \in E_{28}} [\eta_G(u)^2 + \eta_G(v)^2] + \sum_{uv \in E_{29}} [\eta_G(u)^2 + \eta_G(v)^2] + \sum_{uv \in E_{30}} [\eta_G(u)^2 + \eta_G(v)^2] + \sum_{uv \in E_{31}} [\eta_G(u)^2 + \eta_G(v)^2] \\ &+ \sum_{uv \in E_{32}} [\eta_G(u)^2 + \eta_G(v)^2] + \sum_{uv \in E_{33}} [\eta_G(u)^2 + \eta_G(v)^2] + \sum_{uv \in E_{34}} [\eta_G(u)^2 + \eta_G(v)^2] + \sum_{uv \in E_{35}} [\eta_G(u)^2 + \eta_G(v)^2] + \sum_{uv \in E_{36}} [\eta_G(u)^2 + \eta_G(v)^2] \\ &+ \sum_{uv \in E_{37}} [\eta_G(u)^2 + \eta_G(v)^2] + \sum_{uv \in E_{38}} [\eta_G(u)^2 + \eta_G(v)^2] + \sum_{uv \in E_{39}} [\eta_G(u)^2 + \eta_G(v)^2] \end{aligned}$$

Table ii
Edge partition of Abemaciclib drug.

(s, t)	Frequency
(3, 6)	1
(3, 7)	8
(4, 6)	3
(4, 7)	9
(4, 8)	2
(4, 9)	10
(4, 12)	1
(6, 6)	1
(6, 7)	4
(6, 8)	4
(6, 9)	2
(6, 10)	2
(7, 7)	4
(7, 8)	4
(7, 9)	3
(7, 10)	1
(7, 12)	2
(8, 9)	1
(8, 10)	1
(8, 12)	1
(9, 9)	2
(9, 10)	1
(9, 12)	5
(10, 12)	1

$$\begin{aligned} &= [(2^2 + 5^2)(3) + [(3^2 + 6^2)(1) + [(3^2 + 7^2)(18) + [(3^2 + 8^2)(1) + [(4^2 + 6^2)(9) + [(4^2 + 7^2)(10) + [(4^2 + 8^2)(2) \\ &+ [(4^2 + 9^2)(1) + [(4^2 + 10^2)(5) + [(4^2 + 11^2)(5) + [(4^2 + 13^2)(1) + [(5^2 + 10^2)(1) + [(5^2 + 11^2)(1) + [(5^2 + 14^2)(1) + [(6^2 + 7^2)(3) + [(6^2 + 9^2)(1) + [(6^2 + 11^2)(1) \\ &+ [(7^2 + 7^2)(15) + [(7^2 + 8^2)(1) + [(7^2 + 9^2)(6) + [(7^2 + 10^2)(3) + [(7^2 + 11^2)(2) + [(7^2 + 14^2)(1) + [(7^2 + 15^2)(3) + [(8^2 + 8^2)(1) + [(8^2 + 11^2)(2) + [(8^2 + 14^2)(1) + [(9^2 + 9^2)(1) + [(9^2 + 11^2)(1) + [(9^2 + 15^2)(1) + [(10^2 + 11^2)(5) + [(10^2 + 14^2)(1) + [(11^2 + 11^2)(2) + [(11^2 + 13^2)(1) + [(11^2 + 14^2)(2) + [(11^2 + 15^2)(1) + [(13^2 + 14^2)(1) + [(13^2 + 15^2)] \\ &= 14744 \end{aligned}$$

2. By using Eq. (2) and edge partitions given in Table iv we get,

$$M_2^*(G) = \sum_{uv \in E(G)} [\eta_G(u) \cdot \eta_G(v)].$$

Proof. Let G_2 be the graph of Abraxane with vertex set V and edge set

$$\begin{aligned}
 &= \sum_{uv \in E_1} [\eta_G(u) \cdot \eta_G(v)] + \sum_{uv \in E_2} [\eta_G(u) \cdot \eta_G(v)] + \sum_{uv \in E_3} [\eta_G(u) \cdot \eta_G(v)] \\
 &+ \sum_{uv \in E_4} [\eta_G(u) \cdot \eta_G(v)] + \sum_{uv \in E_5} [\eta_G(u) \cdot \eta_G(v)] + \sum_{uv \in E_6} [\eta_G(u) \cdot \eta_G(v)] \\
 &+ \sum_{uv \in E_7} [\eta_G(u) \cdot \eta_G(v)] + \sum_{uv \in E_8} [\eta_G(u) \cdot \eta_G(v)] + \sum_{uv \in E_9} [\eta_G(u) \cdot \eta_G(v)] \\
 &+ \sum_{uv \in E_{10}} [\eta_G(u) \cdot \eta_G(v)] + \sum_{uv \in E_{11}} [\eta_G(u) \cdot \eta_G(v)] + \sum_{uv \in E_{12}} [\eta_G(u) \cdot \eta_G(v)] \\
 &+ \sum_{uv \in E_{13}} [\eta_G(u) \cdot \eta_G(v)] + \sum_{uv \in E_{14}} [\eta_G(u) \cdot \eta_G(v)] + \sum_{uv \in E_{15}} [\eta_G(u) \cdot \eta_G(v)] \\
 &+ \sum_{uv \in E_{16}} [\eta_G(u) \cdot \eta_G(v)] + \sum_{uv \in E_{17}} [\eta_G(u) \cdot \eta_G(v)] + \sum_{uv \in E_{18}} [\eta_G(u) \cdot \eta_G(v)] \\
 &+ \sum_{uv \in E_{19}} [\eta_G(u) \cdot \eta_G(v)] + \sum_{uv \in E_{20}} [\eta_G(u) \cdot \eta_G(v)] + \sum_{uv \in E_{21}} [\eta_G(u) \cdot \eta_G(v)] \\
 &+ \sum_{uv \in E_{22}} [\eta_G(u) \cdot \eta_G(v)] + \sum_{uv \in E_{23}} [\eta_G(u) \cdot \eta_G(v)] + \sum_{uv \in E_{24}} [\eta_G(u) \cdot \eta_G(v)] \\
 &+ \sum_{uv \in E_{25}} [\eta_G(u) \cdot \eta_G(v)] + \sum_{uv \in E_{26}} [\eta_G(u) \cdot \eta_G(v)] + \sum_{uv \in E_{27}} [\eta_G(u) \cdot \eta_G(v)] \\
 &+ \sum_{uv \in E_{28}} [\eta_G(u) \cdot \eta_G(v)] + \sum_{uv \in E_{29}} [\eta_G(u) \cdot \eta_G(v)] + \sum_{uv \in E_{30}} [\eta_G(u) \cdot \eta_G(v)] \\
 &+ \sum_{uv \in E_{31}} [\eta_G(u) \cdot \eta_G(v)] + \sum_{uv \in E_{32}} [\eta_G(u) \cdot \eta_G(v)] + \sum_{uv \in E_{33}} [\eta_G(u) \cdot \eta_G(v)] \\
 &+ \sum_{uv \in E_{34}} [\eta_G(u) \cdot \eta_G(v)] + \sum_{uv \in E_{35}} [\eta_G(u) \cdot \eta_G(v)] + \sum_{uv \in E_{36}} [\eta_G(u) \cdot \eta_G(v)] \\
 &+ \sum_{uv \in E_{37}} [\eta_G(u) \cdot \eta_G(v)] + \sum_{uv \in E_{38}} [\eta_G(u) \cdot \eta_G(v)] + \sum_{uv \in E_{39}} [\eta_G(u) \cdot \eta_G(v)]
 \end{aligned}$$

$$\begin{aligned}
 &= [(2).(5)](3) + [(3).(6)](1) + [(3).(7)](18) + [(3).(8)](1) + [(4).(9)](1) \\
 &+ [(4).(10)](5) + [(4).(11)](5) + [(4).(13)](1) + [(5).(10)](1) \\
 &+ [(5).(11)](1) + [(5).(14)](1) + [(6).(7)](3) + [(6).(9)](1) \\
 &+ [(6).(11)](1) + [(7).(7)](15) + [(7).(8)](1) + [(7).(9)](6) \\
 &+ [(7).(10)](3) + [(7).(11)](2) + [(7).(14)](1) + [(7).(15)](3) \\
 &+ [(8).(8)](1) + [(8).(11)](2) + [(8).(14)](1) + [(9).(9)](1) \\
 &+ [(9).(11)](1) + [(9).(15)](1) + [(10).(11)](5) + [(10).(14)](1) \\
 &+ [(11).(11)](2) + [(11).(13)](1) + [(11).(14)](2) + [(11).(15)](1) \\
 &+ [(13).(14)](1) + [(13).(15)](1) \\
 &= 6504
 \end{aligned}$$

3. By using Eq. (3) and the edge partitions given in Table iv we get

$$HM_N(G) = \sum_{uv \in E(G)} [\eta_G(u) + \eta_G(v)]^2.$$

$$\begin{aligned}
 &= \sum_{uv \in E_1} [\eta_G(u) + \eta_G(v)]^2 + \sum_{uv \in E_2} [\eta_G(u) + \eta_G(v)]^2 + \sum_{uv \in E_3} [\eta_G(u) + \eta_G(v)]^2 + \sum_{uv \in E_4} [\eta_G(u) + \eta_G(v)]^2 + \sum_{uv \in E_5} [\eta_G(u) + \eta_G(v)]^2 \\
 &+ \sum_{uv \in E_6} [\eta_G(u) + \eta_G(v)]^2 + \sum_{uv \in E_7} [\eta_G(u) + \eta_G(v)]^2 + \sum_{uv \in E_8} [\eta_G(u) + \eta_G(v)]^2 + \sum_{uv \in E_9} [\eta_G(u) + \eta_G(v)]^2 + \sum_{uv \in E_{10}} [\eta_G(u) + \eta_G(v)]^2 \\
 &+ \sum_{uv \in E_{11}} [\eta_G(u) + \eta_G(v)]^2 + \sum_{uv \in E_{12}} [\eta_G(u) + \eta_G(v)]^2 + \sum_{uv \in E_{13}} [\eta_G(u) + \eta_G(v)]^2 + \sum_{uv \in E_{14}} [\eta_G(u) + \eta_G(v)]^2 + \sum_{uv \in E_{15}} [\eta_G(u) + \eta_G(v)]^2 \\
 &+ \sum_{uv \in E_{16}} [\eta_G(u) + \eta_G(v)]^2 + \sum_{uv \in E_{17}} [\eta_G(u) + \eta_G(v)]^2 + \sum_{uv \in E_{18}} [\eta_G(u) + \eta_G(v)]^2 + \sum_{uv \in E_{19}} [\eta_G(u) + \eta_G(v)]^2 + \sum_{uv \in E_{20}} [\eta_G(u) + \eta_G(v)]^2 \\
 &+ \sum_{uv \in E_{21}} [\eta_G(u) + \eta_G(v)]^2 + \sum_{uv \in E_{22}} [\eta_G(u) + \eta_G(v)]^2 + \sum_{uv \in E_{23}} [\eta_G(u) + \eta_G(v)]^2 + \sum_{uv \in E_{24}} [\eta_G(u) + \eta_G(v)]^2 + \sum_{uv \in E_{25}} [\eta_G(u) + \eta_G(v)]^2 \\
 &+ \sum_{uv \in E_{26}} [\eta_G(u) + \eta_G(v)]^2 + \sum_{uv \in E_{27}} [\eta_G(u) + \eta_G(v)]^2 + \sum_{uv \in E_{28}} [\eta_G(u) + \eta_G(v)]^2 + \sum_{uv \in E_{29}} [\eta_G(u) + \eta_G(v)]^2 + \sum_{uv \in E_{30}} [\eta_G(u) + \eta_G(v)]^2 \\
 &+ \sum_{uv \in E_{31}} [\eta_G(u) + \eta_G(v)]^2 + \sum_{uv \in E_{32}} [\eta_G(u) + \eta_G(v)]^2 + \sum_{uv \in E_{33}} [\eta_G(u) + \eta_G(v)]^2 + \sum_{uv \in E_{34}} [\eta_G(u) + \eta_G(v)]^2 + \sum_{uv \in E_{35}} [\eta_G(u) + \eta_G(v)]^2 \\
 &+ \sum_{uv \in E_{36}} [\eta_G(u) + \eta_G(v)]^2 + \sum_{uv \in E_{37}} [\eta_G(u) + \eta_G(v)]^2 + \sum_{uv \in E_{38}} [\eta_G(u) + \eta_G(v)]^2 + \sum_{uv \in E_{39}} [\eta_G(u) + \eta_G(v)]^2 \\
 &= [(2 + 5)^2](3) + [(3 + 6)^2](1) + [(3 + 7)^2](18) + [(3 + 8)^2](1) + [(3 + 9)^2](1) + [(4 + 6)^2](9) + [(4 + 7)^2](10) + [(4 + 8)^2](2) \\
 &+ [(4 + 9)^2](1) + [(4 + 10)^2](5) + [(4 + 11)^2](5) + [(4 + 13)^2](1) + [(5 + 10)^2](1) + [(5 + 11)^2](1) + [(5 + 14)^2](1) + [(6 + 7)^2](3) \\
 &+ [(6 + 9)^2](1) + [(6 + 11)^2](1) + [(7 + 7)^2](15) + [(7 + 8)^2](1) + [(7 + 9)^2](6) + [(7 + 10)^2](3) + [(7 + 11)^2](2) + [(7 + 14)^2](1) \\
 &+ [(7 + 15)^2](3) + [(8 + 8)^2](1) + [(8 + 11)^2](2) + [(8 + 14)^2](1) + [(9 + 9)^2](1) + [(9 + 11)^2](1) + [(9 + 15)^2](1) + [(10 + 11)^2](5) \\
 &+ [(10 + 14)^2](1) + [(11 + 11)^2](2) + [(11 + 13)^2](1) + [(11 + 14)^2](2) + [(11 + 15)^2](2) + [(13 + 14)^2](1) + [(13 + 15)^2](1)
 \end{aligned}$$

$$= 27752$$

4 By using Eq. (4) and vertex partitions given in Table iii we get

$$\begin{aligned} M_N(G) &= \sum_{v \in V(G)} [\eta_G(v)]^2 \\ &= \sum_{v \in V_1} [\eta_G(v)]^2 + \sum_{v \in V_2} [\eta_G(v)]^2 + \sum_{v \in V_3} [\eta_G(v)]^2 + \sum_{v \in V_4} [\eta_G(v)]^2 \\ &+ \sum_{v \in V_5} [\eta_G(v)]^2 + \sum_{v \in V_6} [\eta_G(v)]^2 + \sum_{v \in V_7} [\eta_G(v)]^2 + \sum_{v \in V_8} [\eta_G(v)]^2 \\ &+ \sum_{v \in V_9} [\eta_G(v)]^2 + \sum_{v \in V_{10}} [\eta_G(v)]^2 + \sum_{v \in V_{11}} [\eta_G(v)]^2 + \sum_{v \in V_{12}} [\eta_G(v)]^2 \\ &+ \sum_{v \in V_{13}} [\eta_G(v)]^2 \\ &= [(2)^2](3) + [(3)^2](21) + [(4)^2](33) + [(5)^2](3) + [(6)^2](4) \\ &+ [(7)^2](26) + [(8)^2](3) + [(9)^2](4) + [(10)^2](4) + [(11)^2](7) \\ &+ [(13)^2](1) + [(14)^2](2) + [(15)^2](2) \\ &= 4996 \end{aligned}$$

5. By using Eq. (5) and vertex partitions given in Table iii we get

$$\begin{aligned} F_N(G) &= \sum_{v \in V(G)} [\eta_G(v)]^3 \\ &= \sum_{v \in V_1} [\eta_G(v)]^3 + \sum_{v \in V_2} [\eta_G(v)]^3 + \sum_{v \in V_3} [\eta_G(v)]^3 + \sum_{v \in V_4} [\eta_G(v)]^3 \\ &+ \sum_{v \in V_5} [\eta_G(v)]^3 + \sum_{v \in V_6} [\eta_G(v)]^3 + \sum_{v \in V_7} [\eta_G(v)]^3 + \sum_{v \in V_8} [\eta_G(v)]^3 \\ &+ \sum_{v \in V_9} [\eta_G(v)]^3 + \sum_{v \in V_{10}} [\eta_G(v)]^3 + \sum_{v \in V_{11}} [\eta_G(v)]^3 + \sum_{v \in V_{12}} [\eta_G(v)]^3 \\ &+ \sum_{v \in V_{13}} [\eta_G(v)]^3 \\ &= [(2)^3](3) + [(3)^3](21) + [(4)^3](33) + [(5)^3](3) + [(6)^3](4) \\ &+ [(7)^3](26) + [(8)^3](3) + [(9)^3](4) + [(10)^3](4) + [(11)^3](7) \\ &+ [(13)^3](1) + [(14)^3](2) + [(15)^3](2) \\ &= 45064 \end{aligned}$$

Theorem 3. Let G_3 be the graph of Anastrozole, then the topological indices (Eqs. (1)–(5)) for G_3 are given as follows:

1. $F_N^*(G_1) = 4680$
2. $M_2^*(G_1) = 2046$
3. $HM_N(G_1) = 8772$
4. $M_N(G_1) = 1586$
5. $F_N(G_1) = 13106$

Table iii

Vertex partition of Abraxane drug.

$\eta_v(G)$	Frequency
2	3
3	21
4	33
5	3
6	4
7	26
8	3
9	4
10	4
11	7
13	1
14	2
15	2

Table iv

Edge partition of an Abraxane drug.

(s, t)	Frequency
(2, 5)	3
(3, 6)	1
(3, 7)	18
(3, 8)	1
(3, 9)	1
(4, 6)	9
(4, 7)	10
(4, 8)	2
(4, 9)	1
(4, 10)	5
(4, 11)	5
(4, 13)	1
(5, 10)	1
(5, 11)	1
(5, 14)	1
(6, 7)	3
(6, 9)	1
(6, 11)	1
(7, 7)	15
(7, 8)	1
(7, 9)	6
(7, 10)	3
(7, 11)	2
(7, 14)	1
(7, 15)	3
(8, 8)	1
(8, 11)	2
(8, 14)	1
(9, 9)	1
(9, 11)	1
(9, 15)	1
(10, 11)	5
(10, 14)	1
(11, 11)	2
(11, 13)	1
(11, 14)	2
(11, 15)	1
(13, 14)	1
(13, 15)	1

Proof. Let G_3 be the graph of Anastrozole with vertex set V^r and edge set E^r . Let $\eta_v^r(G)$ represent degree of a vertex and $E_{s,t}^r$ represents the class of edges of G_3 joining vertices of degrees s and t. The following tables show the vertex partition and edge partition

1. By using Eq. (1) and edge partitions given in Table vi we get,

$$\begin{aligned}
 F_N^*(G) &= \sum_{uv \in E(G)} [\eta_G(u)^2 + \eta_G(v)^2] = \sum_{uv \in E_1} [\eta_G(u)^2 + \eta_G(v)^2] \\
 &+ \sum_{uv \in E_2} [\eta_G(u)^2 + \eta_G(v)^2] + \sum_{uv \in E_3} [\eta_G(u)^2 + \eta_G(v)^2] \\
 &+ \sum_{uv \in E_4} [\eta_G(u)^2 + \eta_G(v)^2] + \sum_{uv \in E_5} [\eta_G(u)^2 + \eta_G(v)^2] \\
 &+ \sum_{uv \in E_6} [\eta_G(u)^2 + \eta_G(v)^2] \\
 &+ \sum_{uv \in E_7} [\eta_G(u)^2 + \eta_G(v)^2] + \sum_{uv \in E_8} [\eta_G(u)^2 + \eta_G(v)^2] + \sum_{uv \in E_9} [\eta_G(u)^2 + \eta_G(v)^2] \\
 &+ \sum_{uv \in E_{10}} [\eta_G(u)^2 + \eta_G(v)^2] + \sum_{uv \in E_{11}} [\eta_G(u)^2 + \eta_G(v)^2] \\
 &+ \sum_{uv \in E_{12}} [\eta_G(u)^2 + \eta_G(v)^2] + \sum_{uv \in E_{13}} [\eta_G(u)^2 + \eta_G(v)^2] + \sum_{uv \in E_{14}} [\eta_G(u)^2 + \eta_G(v)^2] \\
 &+ \sum_{uv \in E_{15}} [\eta_G(u)^2 + \eta_G(v)^2]
 \end{aligned}$$

$$\begin{aligned}
 &= [(2)^2 + (5)^2](2) + [(3)^2 + (5)^2](1) + [(3)^2 + (6)^2](1) \\
 &\quad + [(3)^2 + (7)^2](3) + [(4)^2 + (7)^2](12) \\
 &\quad + [(4)^2 + (8)^2](2) + [(5)^2 + (6)^2](2) \\
 &\quad + [(5)^2 + (13)^2](2) + [(6)^2 + (6)^2](1) \\
 &\quad + [(6)^2 + (9)^2](2) + [(7)^2 + (10)^2](6) \\
 &\quad + [(7)^2 + (13)^2](4) + [(8)^2 + (9)^2](1) \\
 &\quad + [(8)^2 + (10)^2](1) + [(10)^2 + (3)^2](2)
 \end{aligned}$$

= 4531

2. By using Eq. (2) and edge partitions given in Table vi we get,

$$\begin{aligned}
 M_2^*(G) &= \sum_{uv \in E(G)} [\eta_G(u) \cdot \eta_G(v)]. \\
 &= \sum_{uv \in E_1} [\eta_G(u) \cdot \eta_G(v)] + \sum_{uv \in E_2} [\eta_G(u) \cdot \eta_G(v)] + \sum_{uv \in E_3} [\eta_G(u) \cdot \eta_G(v)] \\
 &\quad + \sum_{uv \in E_4} [\eta_G(u) \cdot \eta_G(v)] + \sum_{uv \in E_5} [\eta_G(u) \cdot \eta_G(v)] \\
 &\quad + \sum_{uv \in E_6} [\eta_G(u) \cdot \eta_G(v)] + \sum_{uv \in E_7} [\eta_G(u) \cdot \eta_G(v)] \\
 &\quad + \sum_{uv \in E_8} [\eta_G(u) \cdot \eta_G(v)] + \sum_{uv \in E_9} [\eta_G(u) \cdot \eta_G(v)] \\
 &\quad + \sum_{uv \in E_{10}} [\eta_G(u) \cdot \eta_G(v)] + \sum_{uv \in E_{11}} [\eta_G(u) \cdot \eta_G(v)] \\
 &\quad + \sum_{uv \in E_{12}} [\eta_G(u) \cdot \eta_G(v)] + \sum_{uv \in E_{13}} [\eta_G(u) \cdot \eta_G(v)] \\
 &\quad + \sum_{uv \in E_{14}} [\eta_G(u) \cdot \eta_G(v)] + \sum_{uv \in E_{15}} [\eta_G(u) \cdot \eta_G(v)] \\
 &= [(2).(5)](2) + [(3).(5)](1) + [(3).(6)](1) + [(3).(7)](3) + [(4).(7)](12) \\
 &\quad + [(4).(8)](2) + [(5).(6)](2) + [(5).(13)](2) + [(6).(6)](1) \\
 &\quad + [(6).(9)](2) + [(7).(10)](6) + [(7).(13)](4) + [(8).(9)](1) \\
 &\quad + [(8).(10)](1) + [(10).(3)](2)
 \end{aligned}$$

= 1976

3. By using Eq. (3) and edge partitions given in Table vi we get

$$\begin{aligned}
 HM_N(G) &= \sum_{uv \in E(G)} [\eta_G(u) + \eta_G(v)]^2. \\
 &= \sum_{uv \in E_1} [\eta_G(u) + \eta_G(v)]^2 + \sum_{uv \in E_2} [\eta_G(u) + \eta_G(v)]^2 + \sum_{uv \in E_3} [\eta_G(u) + \eta_G(v)]^2 \\
 &\quad + \sum_{uv \in E_4} [\eta_G(u) + \eta_G(v)]^2 + \sum_{uv \in E_5} [\eta_G(u) + \eta_G(v)]^2 + \sum_{uv \in E_6} [\eta_G(u) + \eta_G(v)]^2 \\
 &\quad + \sum_{uv \in E_7} [\eta_G(u) + \eta_G(v)]^2 + \sum_{uv \in E_8} [\eta_G(u) + \eta_G(v)]^2 + \sum_{uv \in E_9} [\eta_G(u) + \eta_G(v)]^2 \\
 &\quad + \sum_{uv \in E_{10}} [\eta_G(u) + \eta_G(v)]^2 + \sum_{uv \in E_{11}} [\eta_G(u) + \eta_G(v)]^2 + \sum_{uv \in E_{12}} [\eta_G(u) + \eta_G(v)]^2 \\
 &\quad + \sum_{uv \in E_{13}} [\eta_G(u) + \eta_G(v)]^2 + \sum_{uv \in E_{14}} [\eta_G(u) + \eta_G(v)]^2 + \sum_{uv \in E_{15}} [\eta_G(u) + \eta_G(v)]^2 \\
 &= [(2 + 5)^2](2) + [(3 + 5)^2](1) + [(3 + 6)^2](1) + [(4 + 7)^2](12) \\
 &\quad + [(4 + 8)^2](2) + [(5 + 6)^2](2) + [(5 + 13)^2](2) \\
 &\quad + [(6 + 6)^2](1) + [(6 + 9)^2](2) + [(7 + 10)^2](6) \\
 &\quad + [(7 + 13)^2](4) + [(8 + 9)^2](1) + [(8 + 10)^2](1) \\
 &\quad + [(10 + 13)^2](2)
 \end{aligned}$$

= 8483

4. By using Eq. (4) and vertex partitions given in Table v we get

$$\begin{aligned}
 M_N(G) &= \sum_{v \in V(G)} [\eta_G(v)]^2. \\
 &= \sum_{v \in V_1} [\eta_G(v)]^2 + \sum_{v \in V_2} [\eta_G(v)]^2 + \sum_{v \in V_3} [\eta_G(v)]^2 + \sum_{v \in V_4} [\eta_G(v)]^2 \\
 &\quad + \sum_{v \in V_5} [\eta_G(v)]^2 + \sum_{v \in V_6} [\eta_G(v)]^2 + \sum_{v \in V_7} [\eta_G(v)]^2 + \sum_{v \in V_8} [\eta_G(v)]^2
 \end{aligned}$$

$$\begin{aligned}
 & + \sum_{v \in V_9} [\eta_G(v)]^2 + \sum_{v \in V_{10}} [\eta_G(v)]^2 \\
 & = [(2)^2](2) + [(3)^2](5) + [(4)^2](14) + [(5)^2](3) + [(6)^2](3) + [(7)^2](7) \\
 & + [(8)^2](1) + [(9)^2](1) + [(10)^2](3) + [(13)^2](2) \\
 & = 1586
 \end{aligned}$$

5. By using Eq. (5) and vertex partitions given in Table v we get

$$\begin{aligned}
 F_N(G) &= \sum_{v \in V(G)} [\eta_G(v)]^3. \\
 &= \sum_{v \in V_1} [\eta_G(v)]^3 + \sum_{v \in V_2} [\eta_G(v)]^3 + \sum_{v \in V_3} [\eta_G(v)]^3 + \sum_{v \in V_4} [\eta_G(v)]^3 \\
 &+ \sum_{v \in V_5} [\eta_G(v)]^3 + \sum_{v \in V_6} [\eta_G(v)]^3 + \sum_{v \in V_7} [\eta_G(v)]^3 + \sum_{v \in V_8} [\eta_G(v)]^3 \\
 &+ \sum_{v \in V_9} [\eta_G(v)]^3 + \sum_{v \in V_{10}} [\eta_G(v)]^3 \\
 &= [(2)^3](2) + [(3)^3](5) + [(4)^3](14) + [(5)^3](3) + [(6)^3](3) + [(7)^3](7) \\
 &+ [(8)^3](1) + [(9)^3](1) + [(10)^3](3) + [(13)^3](2) \\
 &= 13106
 \end{aligned}$$

Theorem 4. Let G_4 be the graph of Capecitabine, then the topological indices (Eqs. (1)–(5)) for G_4 are given as follows:

1. $F_N^*(G_1) = 5603$
2. $M_2^*(G_1) = 2429$
3. $HM_N(G_1) = 10461$
4. $M_N(G_1) = 1860$
5. $F_N(G_1) = 14844$

Table v
Vertex partition of an Anastrozole drug.

$\eta_v(G)$	Frequency
2	2
3	5
4	14
5	3
6	3
7	7
8	1
9	1
10	3
13	2

Table vi

Edge partition of an Anastrozole drug.

(s, t)	Frequency
(2, 5)	2
(3, 5)	1
(3, 6)	1
(3, 7)	3
(4, 7)	12
(4, 8)	2
(5, 6)	2
(5, 13)	2
(6, 6)	1
(6, 9)	2
(7, 10)	5
(7, 13)	4
(8, 9)	1
(8, 10)	1
(10, 13)	2

Proof. Let G_4 be the graph of Capecitabine with vertex set V^r and edge set E^r . Let $\eta_v^r(G)$ represent the degree of a vertex and $E_{s,t}^r$ represents the class of edges of G_4 joining vertices of degrees s and t . The following tables show the vertex partition and edge partition

1. By using Eq. (1) and edge partitions given in Table viii we get,

$$\begin{aligned}
 F_N^*(G) &= \sum_{uv \in E(G)} [\eta_G(u)^2 + \eta_G(v)^2]. \\
 &= \sum_{uv \in E_1} [\eta_G(u)^2 + \eta_G(v)^2] + \sum_{uv \in E_2} [\eta_G(u)^2 + \eta_G(v)^2] + \sum_{uv \in E_3} [\eta_G(u)^2 + \eta_G(v)^2] \\
 &+ \sum_{uv \in E_4} [\eta_G(u)^2 + \eta_G(v)^2] + \sum_{uv \in E_5} [\eta_G(u)^2 + \eta_G(v)^2] + \sum_{uv \in E_6} [\eta_G(u)^2 + \eta_G(v)^2] \\
 &+ \sum_{uv \in E_7} [\eta_G(u)^2 + \eta_G(v)^2] + \sum_{uv \in E_8} [\eta_G(u)^2 + \eta_G(v)^2] + \sum_{uv \in E_9} [\eta_G(u)^2 + \eta_G(v)^2] \\
 &+ \sum_{uv \in E_{10}} [\eta_G(u)^2 + \eta_G(v)^2] + \sum_{uv \in E_{11}} [\eta_G(u)^2 + \eta_G(v)^2] + \sum_{uv \in E_{12}} [\eta_G(u)^2 + \eta_G(v)^2] \\
 &+ \sum_{uv \in E_{13}} [\eta_G(u)^2 + \eta_G(v)^2] + \sum_{uv \in E_{14}} [\eta_G(u)^2 + \eta_G(v)^2] + \sum_{uv \in E_{15}} [\eta_G(u)^2 + \eta_G(v)^2] \\
 &+ \sum_{uv \in E_{16}} [\eta_G(u)^2 + \eta_G(v)^2] + \sum_{uv \in E_{17}} [\eta_G(u)^2 + \eta_G(v)^2] + \sum_{uv \in E_{18}} [\eta_G(u)^2 + \eta_G(v)^2] \\
 &+ \sum_{uv \in E_{19}} [\eta_G(u)^2 + \eta_G(v)^2] + \sum_{uv \in E_{20}} [\eta_G(u)^2 + \eta_G(v)^2] + \sum_{uv \in E_{21}} [\eta_G(u)^2 + \eta_G(v)^2] \\
 &+ \sum_{uv \in E_{22}} [\eta_G(u)^2 + \eta_G(v)^2] \\
 &= [(2)^2 + (5)^2](1) + [(3)^2 + (6)^2](2) + [(3)^2 + (7)^2](3) \\
 &+ [(4)^2 + (5)^2](1) + [(4)^2 + (7)^2](6) + [(4)^2 + (8)^2](2) \\
 &+ [(4)^2 + (10)^2](8) + [(4)^2 + (3)^2](11) + [(5)^2 + (11)^2](2) \\
 &+ [(6)^2 + (6)^2](1) + [(6)^2 + (7)^2](2) + [(6)^2 + (8)^2](1)
 \end{aligned}$$

$$\begin{aligned}
 &+ [(6)^2 + (10)^2](1) + [(7)^2 + (7)^2](1) + [(7)^2 + (8)^2](2) \\
 &+ [(7)^2 + (10)^2](2) + [(7)^2 + (11)^2](1) + [(8)^2 + (10)^2](2) \\
 &+ [(8)^2 + (11)^2](1) + [(10)^2 + (10)^2](3) + [(10)^2 + (11)^2](1) \\
 &+ [(11)^2 + (11)^2](2) \\
 &= 5603
 \end{aligned}$$

2. By using Eq. (2) and edge partitions given in Table viii we get,

$$\begin{aligned}
 M_2^*(G) &= \sum_{uv \in E(G)} [\eta_G(u) \cdot \eta_G(v)]. \\
 &= \sum_{uv \in E_1} [\eta_G(u) \cdot \eta_G(v)] + \sum_{uv \in E_2} [\eta_G(u) \cdot \eta_G(v)] + \sum_{uv \in E_3} [\eta_G(u) \cdot \eta_G(v)] \\
 &+ \sum_{uv \in E_4} [\eta_G(u) \cdot \eta_G(v)] + \sum_{uv \in E_5} [\eta_G(u) \cdot \eta_G(v)] + \sum_{uv \in E_6} [\eta_G(u) \cdot \eta_G(v)] \\
 &+ \sum_{uv \in E_7} [\eta_G(u) \cdot \eta_G(v)] + \sum_{uv \in E_8} [\eta_G(u) \cdot \eta_G(v)] + \sum_{uv \in E_9} [\eta_G(u) \cdot \eta_G(v)] \\
 &+ \sum_{uv \in E_{10}} [\eta_G(u) \cdot \eta_G(v)] + \sum_{uv \in E_{11}} [\eta_G(u) \cdot \eta_G(v)] + \sum_{uv \in E_{12}} [\eta_G(u) \cdot \eta_G(v)] \\
 &+ \sum_{uv \in E_{13}} [\eta_G(u) \cdot \eta_G(v)] + \sum_{uv \in E_{14}} [\eta_G(u) \cdot \eta_G(v)] + \sum_{uv \in E_{15}} [\eta_G(u) \cdot \eta_G(v)] \\
 &+ \sum_{uv \in E_{16}} [\eta_G(u) \cdot \eta_G(v)] + \sum_{uv \in E_{17}} [\eta_G(u) \cdot \eta_G(v)] + \sum_{uv \in E_{18}} [\eta_G(u) \cdot \eta_G(v)] \\
 &+ \sum_{uv \in E_{19}} [\eta_G(u) \cdot \eta_G(v)] + \sum_{uv \in E_{20}} [\eta_G(u) \cdot \eta_G(v)] + \sum_{uv \in E_{21}} [\eta_G(u) \cdot \eta_G(v)] \\
 &+ \sum_{uv \in E_{22}} [\eta_G(u) \cdot \eta_G(v)] = [(2) \cdot (5)](1) + [(3) \cdot (6)](2) + [(3) \cdot (7)](3) \\
 &+ [(4) \cdot (5)](1) + [(4) \cdot (7)](6) + [(4) \cdot (8)](2) + [(4) \cdot (10)](8) \\
 &+ [(4) \cdot (11)](3) + [(5) \cdot (11)](2) + [(6) \cdot (6)](1) + [(6) \cdot (7)](2) \\
 &+ [(6) \cdot (8)](1) + [(6) \cdot (10)](1) + [(7) \cdot (7)](1) + [(7) \cdot (8)](2) \\
 &+ [(7) \cdot (10)](2) + [(7) \cdot (11)](1) + [(8) \cdot (10)](2) + [(8) \cdot (11)](1) \\
 &+ [(10) \cdot (10)](3) + [(10) \cdot (11)](1) + [(11) \cdot (11)](2) \\
 &= 2429
 \end{aligned}$$

3. By using Eq. (3) and the edge partitions given in Table viii we get

$$\begin{aligned}
 HM_N(G) &= \sum_{uv \in E(G)} [\eta_G(u) + \eta_G(v)]^2. \\
 &= \sum_{uv \in E_1} [\eta_G(u) + \eta_G(v)]^2 + \sum_{uv \in E_2} [\eta_G(u) + \eta_G(v)]^2 + \sum_{uv \in E_3} [\eta_G(u) + \eta_G(v)]^2 \\
 &+ \sum_{uv \in E_4} [\eta_G(u) + \eta_G(v)]^2 + \sum_{uv \in E_5} [\eta_G(u) + \eta_G(v)]^2 + \sum_{uv \in E_6} [\eta_G(u) + \eta_G(v)]^2
 \end{aligned}$$

$$\begin{aligned}
 &+ \sum_{uv \in E_7} [\eta_G(u) + \eta_G(v)]^2 + \sum_{uv \in E_8} [\eta_G(u) + \eta_G(v)]^2 + \sum_{uv \in E_9} [\eta_G(u) + \eta_G(v)]^2 \\
 &+ \sum_{uv \in E_{10}} [\eta_G(u) + \eta_G(v)]^2 + \sum_{uv \in E_{11}} [\eta_G(u) + \eta_G(v)]^2 + \sum_{uv \in E_{12}} [\eta_G(u) + \eta_G(v)]^2 \\
 &+ \sum_{uv \in E_{13}} [\eta_G(u) + \eta_G(v)]^2 + \sum_{uv \in E_{14}} [\eta_G(u) + \eta_G(v)]^2 + \sum_{uv \in E_{15}} [\eta_G(u) + \eta_G(v)]^2 \\
 &+ \sum_{uv \in E_{16}} [\eta_G(u) + \eta_G(v)]^2 + \sum_{uv \in E_{17}} [\eta_G(u) + \eta_G(v)]^2 + \sum_{uv \in E_{18}} [\eta_G(u) + \eta_G(v)]^2 \\
 &+ \sum_{uv \in E_{19}} [\eta_G(u) + \eta_G(v)]^2 + \sum_{uv \in E_{20}} [\eta_G(u) + \eta_G(v)]^2 + \sum_{uv \in E_{21}} [\eta_G(u) + \eta_G(v)]^2 \\
 &+ \sum_{uv \in E_{22}} [\eta_G(u) + \eta_G(v)]^2 \\
 &= [(2 + 5)^2](1) + [(3 + 6)^2](2) + [(3 + 7)^2](3) + [(4 + 5)^2](1) \\
 &+ [(4 + 7)^2](6) + [(4 + 8)^2](2) + [(4 + 10)^2](8) + [(4 + 11)^2](3) \\
 &+ [(5 + 11)^2](2) + [(6 + 6)^2](1) + [(6 + 7)^2](2) + [(6 + 8)^2](1) \\
 &+ [(6 + 10)^2](1) + [(7 + 7)^2](1) + [(7 + 8)^2](2) + [(7 + 10)^2](2) \\
 &+ [(7 + 11)^2](1) + [(8 + 10)^2](2) + [(8 + 11)^2](1) + [(10 + 10)^2](3) \\
 &+ [(10 + 11)^2](1) + [(11 + 11)^2](2) \\
 &= 10461
 \end{aligned}$$

4. By using Eq. (4) and vertex partitions given in Table vii we get

$$\begin{aligned}
 M_N(G) &= \sum_{v \in V(G)} [\eta_G(v)]^2. \\
 &= \sum_{v \in V_1} [\eta_G(v)]^2 + \sum_{v \in V_2} [\eta_G(v)]^2 + \sum_{v \in V_3} [\eta_G(v)]^2 + \sum_{v \in V_4} [\eta_G(v)]^2 \\
 &+ \sum_{v \in V_5} [\eta_G(v)]^2 + \sum_{v \in V_6} [\eta_G(v)]^2 + \sum_{v \in V_7} [\eta_G(v)]^2 + \sum_{v \in V_8} [\eta_G(v)]^2 \\
 &+ \sum_{v \in V_9} [\eta_G(v)]^2 \\
 &= [(2)^2](1) + [(3)^2](5) + [(4)^2](19) + [(5)^2](2) + [(6)^2](3) \\
 &+ [(7)^2](6) + [(8)^2](3) + [(10)^2](5) + [(11)^2](3) \\
 &= 1860
 \end{aligned}$$

5. By using Eq. (5) and vertex partitions given in Table vii we get

Table 1
Numerical values of the computed TIs for 14 considered drugs.

Name of Drugs	$M_N(G)$	$F_N(G)$	$F_N^*(G)$	$M_2^*(G)$	$HM_N(G)$
Abemaciclib	2776	21806	8018	3613	15244
Abraxane	4996	45064	14744	6504	27752
Anastrozole	1586	13106	4680	2046	8772
Capecitabine	1860	14844	5603	2429	10461
Cyclophosphamide	1156	9198	3428	1509	6446
Everolimus	6311	54001	19419	8436	36291
Exemestane	2395	22927	2779	3215	13819
Fulvestrant	4117	38481	13830	5907	25644
Ixabepilone	2922	28760	10377	4469	19315
Letrozole	1180	8748	3308	1515	6338
Megestrol Acetate	2751	25673	7811	3388	14587
Methotrexate	1814	12688	5026	2276	9578
Tamoxifen	2069	15293	5762	2617	10996
Thiotepa	1226	11390	3848	1723	7294

$$\begin{aligned}
 F_N(G) &= \sum_{v \in V(G)} [\eta_G(v)]^3 \\
 &= \sum_{v \in V_1} [\eta_G(v)]^3 + \sum_{v \in V_2} [\eta_G(v)]^3 + \sum_{v \in V_3} [\eta_G(v)]^3 + \sum_{v \in V_4} [\eta_G(v)]^3 \\
 &\quad + \sum_{v \in V_5} [\eta_G(v)]^3 + \sum_{v \in V_6} [\eta_G(v)]^3 + \sum_{v \in V_7} [\eta_G(v)]^3 + \sum_{v \in V_8} [\eta_G(v)]^3 \\
 &\quad + \sum_{v \in V_9} [\eta_G(v)]^3 \\
 &= [(2)^3](1) + [(3)^3](5) + [(4)^3](19) + [(5)^3](2) + [(6)^3](3) \\
 &\quad + [(7)^3](6) + [(8)^3](3) + [(10)^3](5) + [(11)^3](3) \\
 &= 14844
 \end{aligned}$$

Table 2
Physical properties of drugs.

Name of drugs	BP (°C at 760 mmHg)	MP (°C)	Enthalpy (kJmol ⁻¹)	Flash point (°C)	MR	MV (cm ³)	P 10-24 (cm ³)
Abemaciclib	689.3		101	370.7	140.4	382.3	55.7
Abraxane	957.1		146	532.6	219.3	610.6	86.9
Anastrozole	469.7	81.5	73.2	237.9	90	270.3	35.7
Capecitabine	517	115.5			82.3	240.5	32.6
Cyclophosphamide	336.1	51	57.9	157.1	58.1	195.7	23
Everolimus	998.7	998.7	165.1	557.8	257.7	811.2	102.2
Exemestane	453.7	155.13	71.3	169	85.8	260.6	34
Fulvestrant	674.8	105	104.1	361.9	154	505.1	61.1
Ixabepilone	697.8		107.3	375.8	140.1	451.6	55.5
Letrozole	563.5	181	84.7	294.6	87.1	234.5	34.5
Megestrol Acetate	507.1	214	77.7	218.5	106.4	333.4	42.2
Methotrexate		192			119	295.7	47.2
Tamoxifen	482.3	96	74.7	140	118.9	118.9	47.1
Thiotepa	270.2	51.5	50.8	117.2	49.1	125.8	19.5

Table 3
The correlation coefficients of the experimental physical properties and computed TI values of drugs.

Topological index	Correlation coefficients of BP	Correlation coefficients of MP	Correlation coefficients of enthalpy	Correlation coefficients of FP	Correlation coefficients of MR	Correlation coefficients of MV	Correlation coefficients of P
FN*(G)	0.90	0.79	0.93	0.88	0.94	0.94	0.94
M2*(G)	0.90	0.82	0.93	0.87	0.94	0.95	0.94
HMN(G)	0.90	0.81	0.92	0.86	0.94	0.95	0.94
MN(G)	0.91	0.84	0.93	0.86	0.95	0.95	0.95
FN(G)	0.88	0.79	0.91	0.85	0.92	0.94	0.92

Theorem 5. Let G_5 be the graph of Cyclophosphamide, then the topological indices (Eqs. (1)–(5)) for G_5 are given as follows:

- $F_N^*(G_1) = 3428$
- $M_2^*(G_1) = 1509$
- $HM_N(G_1) = 6446$
- $M_N(G_1) = 1156$
- $F_N(G_1) = 9198$

Table vii
Vertex partition of a Capecitabine drug.

$\eta_v(G)$	Frequency
2	1
3	5
4	19
5	2
6	3
7	6
8	3
10	5
11	3

Table viii
Edge partition of a Capecitabine drug.

(s, t)	Frequency
(2, 5)	1
(3, 6)	2
(3, 7)	3
(4, 5)	1
(4, 7)	6
(4, 8)	2

(continued on next page)

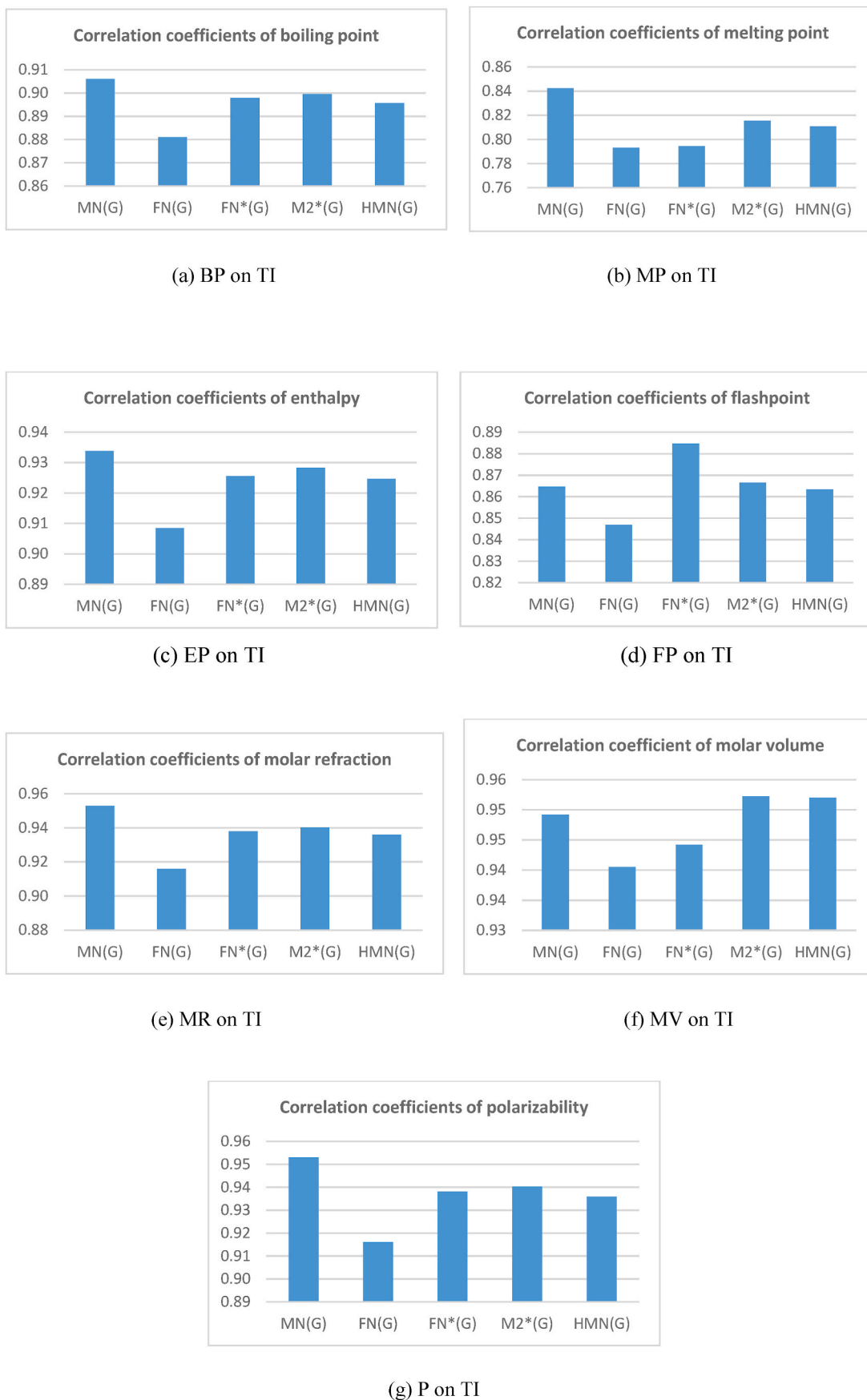


Fig. 2. Correlation coefficients of physical properties and Topological indices (TIs).

Table 4

Statistical Parameters for the linear QSPR model for $F_N^*(G)$. The bold font indicates the maximum correlation value.

Physical property	N	A	b	r	r ²	F	P
Boiling point	13	290.227	0.037	0.898	0.806	45.765	0.000
Melting point	11	-79.851	0.041	0.794	0.631	15.404	0.393
Enthalpy	12	39.483	0.003	0.926	0.857	59.766	0.000
Flash point	12	95.358	0.024	0.885	0.783	36.014	0.035
Molar Refraction	14	37.990	0.011	0.940	0.884	91.649	0.002
Molar Volume	14	65.429	0.036	0.952	0.891	98.544	0.073
Polarizability	14	15.047	0.004	0.938	0.880	87.944	0.004

Table 5

Statistical parameters for the linear QSPR model for $M_2^*(G)$. The bold font indicates the highest correlation value.

Physical property	N	A	b	r	r ²	F	P
Boiling point	13	257.017	0.090	0.899	0.809	46.604	0.001
Melting point	11	-123.529	0.103	0.816	0.665	17.875	0.212
Enthalpy	12	38.784	0.014	0.928	0.862	62.362	0.001
Flash point	12	76.128	0.058	0.867	0.751	30.143	0.126
Molar Refraction	14	28.842	0.026	0.941	0.884	91.326	0.024
Molar Volume	14	33.042	0.088	0.952	0.907	116.658	0.340
Polarizability	14	11.421	0.010	0.940	0.884	91.531	0.024

Table 6

Statistical parameters used for the linear QSPR model for $HM_N(G)$. The bold font indicates the highest correlation value.

Physical property	N	A	b	r	r ²	F	P
Boiling point	13	261.120	0.021	0.896	0.802	44.597	0.001
Melting point	11	-117.725	0.024	0.811	0.657	17.258	0.234
Enthalpy	12	41.740	0.003	0.925	0.855	59.005	0.001
Flash point	12	78.877	0.013	0.863	0.746	29.300	0.116
Molar Refraction	14	30.173	0.006	0.936	0.876	84.539	0.022
Molar Volume	14	36.143	0.020	0.952	0.906	116.081	0.296
Polarizability	14	11.948	0.002	0.936	0.876	84.722	0.022

Table 7

Statistical parameters used for the linear QSPR model for $M_N(G)$. The bold font indicates the highest correlation value.

Physical property	N	A	b	r	r ²	F	P
Boiling point	13	249.201	0.124	0.906	0.821	50.432	0.001
Melting point	11	-147.316	0.146	0.842	0.710	22.006	0.128
Enthalpy	12	37.718	0.020	0.934	0.872	68.104	0.001
Flash point	12	73.612	0.079	0.865	0.748	29.615	0.144
Molar Refraction	14	25.462	0.036	0.953	0.908	118.362	0.028
Molar Volume	14	27.063	0.120	0.949	0.789	44.827	0.083
Polarizability	14	10.080	0.014	0.953	0.908	118.698	0.028

Table 8

Statistical parameters used for the linear QSPR model for $F_N(G)$. The bold font indicates the highest correlation value.

Physical property	N	A	b	r	r ²	F	P
Boiling point	13	272.117	0.013	0.881	0.776	38.118	0.001
Melting point	11	-106.954	0.015	0.793	0.629	15.257	0.290
Enthalpy	12	40.970	0.002	0.908	0.825	47.216	0.001
Flash point	12	85.222	0.009	0.847	0.717	25.362	0.106
Molar Refraction	14	34.803	0.004	0.916	0.839	62.472	0.019
Molar Volume	14	48.980	0.013	0.941	0.885	91.952	0.198
Polarizability	14	13.785	0.002	0.916	0.839	62.558	0.019

Table viii (continued)

(s, t)	Frequency
(4, 10)	8
(4, 11)	3
(5, 11)	2
(6, 6)	1
(6, 7)	2
(6, 8)	1

(continued on next column)

Table viii (continued)

(s, t)	Frequency
(6, 10)	1
(7, 7)	1
(7, 8)	2
(7, 10)	2
(7, 11)	1
(8, 10)	2

(continued on next page)

Table 9
Standard error of estimate.

Topological index	Std. error of the estimate for boiling point	Std. error of the estimate for melting point	Std. error of the estimate for enthalpy	Std. error of the estimate for flash point	Std. error of the estimate for molar refraction	Std. error of the estimate for molar volume	Std. error of the estimate for Polarizability
FN*(G)	98.84	172.44	13.60	72.50	21.09	66.31	8.35
M2*(G)	98.12	164.32	13.36	77.63	20.72	61.47	8.21
HMN(G)	99.87	166.24	13.68	78.45	21.44	61.61	8.49
MN(G)	95.01	152.98	12.86	78.14	18.45	63.37	7.31
FN(G)	106.25	172.96	15.02	82.71	24.41	68.38	9.67

Table 10
Comparison of experimental and calculated values for boiling point from linear regression models.

Name of drugs	The boiling point of drugs	Boiling point computed from regression model for $M_N(G)$	Boiling point computed from regression model for $F_N(G)$	Boiling point computed from regression model for $F_N^*(G)$	Boiling point computed from regression model for $M_N^*(G)$	Boiling point computed from regression model for $HM_N(G)$
Abemaciclib	689.3 ± 65.0 °C at 760 mmHg	593.025	559.754	587.736	583.155	578.285
Abraxane	957.1 ± 65.0 °C at 760 mmHg	867.985	866.545	837.304	844.119	838.525
Anastrozole	469.7 ± 55.0 °C at 760 mmHg	445.636	444.995	463.879	441.705	443.629
Capecitabine	517 °C at 760 mmHg	479.573	467.920	498.127	476.278	478.770
Cyclophosphamide	336.1 ± 52.0 °C at 760 mmHg	392.378	393.445	417.423	393.231	395.235
Everolimus	998.7 ± 75.0 °C at 760 mmHg	1030.856	984.431	1010.771	1018.516	1016.186
Exemestane	453.7 ± 45.0 °C at 760 mmHg	545.836	574.541	393.342	547.228	548.636
Fulvestrant	674.8 ± 55.0 °C at 760 mmHg	759.116	779.710	803.390	790.229	794.666
Ixabepilone	697.8 ± 55.0 °C at 760 mmHg	611.108	651.483	675.267	660.424	662.985
Letrozole	563.5 ± 60.0 °C at 760 mmHg	395.351	387.509	412.971	393.773	392.988
Megestrol Acetate	507.1 ± 50.0 °C at 760 mmHg	589.929	610.763	580.055	562.845	564.615
Tamoxifen	482.3 ± 33.0 °C at 760 mmHg	505.459	473.843	504.027	493.248	489.901
Thiotepa	270.2 ± 23.0 °C at 760 mmHg	401.048	422.359	433.008	412.549	412.878

Table 11
Comparison of experimental and calculated values for melting point from linear regression models.

Name of drugs	The melting point of drugs	Melting point computed from regression model for $M_N(G)$	Melting point computed from regression model for $F_N(G)$	Melting point computed from regression model for $F_N^*(G)$	Melting point computed from regression model for $M_N^*(G)$	Melting point computed from regression model for $HM_N(G)$
Anastrozole	81.5	84.115	90.944	113.544	86.559	88.767
Capecitabine	115.5	124.098	117.187	151.686	125.887	128.526
Cyclophosphamide	51	21.369	31.934	61.806	31.419	34.013
Everolimus	998.7	773.592	708.451	722.615	742.700	736.562
Exemestane	155.13	202.165	239.239	34.987	206.595	207.573
Fulvestrant	105	453.442	474.101	491.656	483.016	485.933
Letrozole	181	24.871	25.139	56.848	32.035	31.471
Megestrol Acetate	214	254.113	280.703	242.928	224.359	225.652
Methotrexate	192	117.385	84.632	127.842	110.176	107.740
Tamoxifen	96	154.595	123.967	158.256	145.191	141.120
Thiotepa	51.5	31.584	65.033	79.162	53.393	53.975

Table viii (continued)

(s, t)	Frequency
(8, 11)	1
(10, 10)	3
(10, 11)	1
(11, 11)	2

and edge set E^v . Let $\eta_v^v(G)$ represent the degree of a vertex and represent the class of edges of G_5 joining vertices of degrees s and t. The following tables show the vertex partition and edge partition

1. By using Eq. (1) and edge partitions given in Table x we get,

$$F_N^*(G) = \sum_{w \in E(G)} [\eta_G(u)^2 + \eta_G(v)^2].$$

Proof. Let G_5 be the graph of Cyclophosphamide with vertex set V^v

Table 12
Comparison of experimental and calculated values for enthalpy from regression models.

Name of drugs	Enthalpy of drugs	Enthalpy computed from regression model for $M_N(G)$	Enthalpy computed from regression model for $F_N(G)$	Enthalpy computed from regression model for $F_N^*(G)$	Enthalpy computed from regression model for $M_N^*(G)$	Enthalpy computed from regression model for $HM_N(G)$
Abemaciclib	101.0 ± 3.0 kJ/mol	92.532	87.046	66.141	90.910	89.946
Abraxane	146.0 ± 3.0 kJ/mol	136.367	136.189	88.503	132.619	129.500
Anastrozole	73.2 ± 3.0 kJ/mol	69.035	68.663	55.043	68.302	69.479
Cyclophosphamide	57.9 ± 3.0 kJ/mol	60.544	60.405	50.880	60.555	62.124
Everolimus	165.1 ± 6.0 kJ/mol	162.333	155.073	104.046	160.493	156.503
Exemestane	71.3 ± 3.0 kJ/mol	85.009	89.414	48.722	85.168	85.440
Fulvestrant	104.1 ± 3.0 kJ/mol	119.011	122.280	85.464	124.006	122.834
Ixabepilone	107.3 ± 3.0 kJ/mol	95.415	101.739	73.984	103.260	102.820
Letrozole	84.7 ± 3.0 kJ/mol	61.018	59.454	50.481	60.641	61.782
Megestrol Acetate	77.7 ± 3.0 kJ/mol	92.038	95.216	65.452	87.664	87.868
Tamoxifen	74.7 ± 3.0 kJ/mol	78.572	73.284	58.640	76.540	76.512
Thiotepa	50.8 ± 3.0 kJ/mol	61.926	65.037	52.276	63.642	64.805

Table 13
Comparison of experimental and calculated values for flash point from regression models.

Name of drugs	The flash point of drugs	Flash point computed from regression model for $M_N(G)$	Flash point computed from regression model for $F_N(G)$	Flash point computed from regression model for $F_N^*(G)$	Flash point computed from regression model for $M_N^*(G)$	Flash point computed from regression model for $HM_N(G)$
Abemaciclib	370.7 ± 34.3 °C	293.284	271.139	290.793	286.721	283.709
Abraxane	532.6 ± 34.3 °C	468.959	469.435	454.736	455.231	451.778
Anastrozole	237.9 ± 31.5 °C	199.116	196.963	209.431	195.384	196.746
Cyclophosphamide	157.1 ± 30.7 °C	165.089	163.644	178.914	164.084	165.491
Everolimus	557.8 ± 37.1 °C	573.018	545.631	568.687	567.843	566.515
Exemestane	169.0 ± 25.7 °C	263.135	280.696	163.095	263.523	264.562
Fulvestrant	361.9 ± 31.5 °C	399.401	413.308	432.458	420.433	423.453
Ixabepilone	375.8 ± 31.5 °C	304.838	330.428	348.293	336.616	338.411
Letrozole	294.6 ± 32.9 °C	166.989	159.807	175.989	164.434	164.040
Megestrol Acetate	218.5 ± 30.2 °C	291.306	304.108	285.748	273.607	274.881
Tamoxifen	140.0 ± 27.7 °C	237.337	215.609	235.804	228.667	226.629
Thiotepa	117.2 ± 22.6 °C	170.629	182.333	189.152	176.557	176.886

Table 14
Comparison of actual and calculated values for molar refraction(MR) from regression models.

Name of drugs	Molar refraction of drugs	Molar refraction computed from regression model for $M_N(G)$	Molar refraction computed from regression model for $F_N(G)$	Molar refraction computed from regression model for $F_N^*(G)$	Molar refraction computed from regression model for $M_N^*(G)$	Molar refraction computed from regression model for $HM_N(G)$
Abemaciclib	140.4 ± 0.5 cm ³	126.444	117.492	124.813	123.769	122.394
Abraxane	219.3 ± 0.4 cm ³	207.201	205.687	197.646	199.726	198.064
Anastrozole	90.0 ± 0.5 cm ³	83.156	84.502	88.668	82.598	83.241
Capecitabine	82.3 ± 0.5 cm ³	93.123	91.092	98.662	92.661	93.458
Cyclophosphamide	58.1 ± 0.4 cm ³	67.514	69.682	75.110	68.489	69.169
Everolimus	257.7 ± 0.4 cm ³	255.037	239.577	248.270	250.487	249.722
Exemestane	85.8 ± 0.4 cm ³	112.585	121.743	68.083	113.312	113.773
Fulvestrant	154.0 ± 0.3 cm ³	175.226	180.725	187.749	184.041	185.311
Ixabepilone	140.1 ± 0.3 cm ³	131.756	143.862	150.358	146.259	147.022
Letrozole	87.1 ± 0.5 cm ³	68.387	67.976	73.811	68.647	68.516
Megestrol Acetate	106.4 ± 0.4 cm ³	125.535	132.156	122.572	117.857	118.419
Methotrexate	119.0 ± 0.3 cm ³	91.450	82.916	92.414	88.641	88.117
Tamoxifen	118.9 ± 0.3 cm ³	100.726	92.795	100.384	97.600	96.695
Thiotepa	49.1 ± 0.4 cm ³	70.060	77.994	79.658	74.112	74.299

$$\begin{aligned}
 &= \sum_{uv \in E_1} [\eta_G(u)^2 + \eta_G(v)^2] + \sum_{uv \in E_2} [\eta_G(u)^2 + \eta_G(v)^2] + \sum_{uv \in E_3} [\eta_G(u)^2 + \eta_G(v)^2] \\
 &+ \sum_{uv \in E_4} [\eta_G(u)^2 + \eta_G(v)^2] + \sum_{uv \in E_5} [\eta_G(u)^2 + \eta_G(v)^2] + \sum_{uv \in E_6} [\eta_G(u)^2 + \eta_G(v)^2] \\
 &+ \sum_{uv \in E_7} [\eta_G(u)^2 + \eta_G(v)^2] + \sum_{uv \in E_8} [\eta_G(u)^2 + \eta_G(v)^2] + \sum_{uv \in E_9} [\eta_G(u)^2 + \eta_G(v)^2] \\
 &+ \sum_{uv \in E_{10}} [\eta_G(u)^2 + \eta_G(v)^2] + \sum_{uv \in E_{11}} [\eta_G(u)^2 + \eta_G(v)^2] \\
 &+ \sum_{uv \in E_{12}} [\eta_G(u)^2 + \eta_G(v)^2] \\
 &= [(3)^2 + (9)^2](1) + [(4)^2 + (7)^2](6) + [(4)^2 + (8)^2](2) \\
 &+ [(4)^2 + (9)^2](7) + [(4)^2 + (10)^2](2) + [(7)^2 + (9)^2](2)
 \end{aligned}$$

Table 15
Comparison of experimental and calculated values for molar volume from the regression models.

Name of drugs	Molar volume of drugs	Molar volume computed from regression model for $M_N(G)$	Molar volume computed from regression model for $F_N(G)$	Molar volume computed from regression model for $F_N^*(G)$	Molar volume computed from regression model for $M_N^*(G)$	Molar volume computed from regression model for $HM_N(G)$
Abemaciclib	382.3 ± 7.0 cm3	360.051	330.071	354.771	351.326	346.722
Abraxane	610.6 ± 5.0 cm3	626.346	629.879	597.490	606.006	601.559
Anastrozole	270.3 ± 7.0 cm3	217.308	217.923	234.314	213.283	214.862
Capecitabine	240.5 ± 7.0 cm3	250.175	240.327	267.622	247.023	249.274
Cyclophosphamide	195.7 ± 5.0 cm3	165.728	167.547	189.134	165.976	167.473
Everolimus	811.2 ± 5.0 cm3	784.084	745.081	766.195	776.204	775.531
Exemestane	260.6 ± 5.0 cm3	314.349	344.521	165.713	316.265	317.689
Fulvestrant	505.1 ± 3.0 cm3	520.908	545.020	564.507	553.414	558.610
Ixabepilone	451.6 ± 3.0 cm3	377.564	419.712	439.900	426.735	429.664
Letrozole	234.5 ± 7.0 cm3	168.607	161.747	184.803	166.505	165.272
Megestrol Acetate	333.4 ± 5.0 cm3	357.053	379.919	347.301	331.505	333.336
Methotrexate	295.7 ± 3.0 cm3	244.657	212.535	246.800	233.545	231.284
Tamoxifen	118.9 ± 0.3 cm3	275.245	246.115	273.360	263.585	260.174
Thiotepa	125.8 ± 5.0 cm3	174.125	195.803	204.290	184.829	184.750

Table 16
Comparison of experimental and calculated values for polarizability from the regression models.

Name of drugs	Polarizability of drugs	polarizability computed from regression model for $M_N(G)$	polarizability computed from regression model for $F_N(G)$	polarizability computed from regression model for $F_N^*(G)$	polarizability computed from regression model for $M_N^*(G)$	polarizability computed from regression model for $HM_N(G)$
Abemaciclib	55.7 ± 0.5 10-24cm3	50.128	46.578	49.482	49.067	48.522
Abraxane	86.9 ± 0.5 10-24cm3	82.155	81.554	78.367	79.191	78.532
Anastrozole	35.7 ± 0.5 10-24cm3	32.961	33.495	35.146	32.740	32.994
Capecitabine	32.6 ± 0.5 10-24cm3	36.914	36.108	39.110	36.730	37.047
Cyclophosphamide	23.0 ± 0.5 10-24cm3	26.757	27.618	29.769	27.144	27.414
Everolimus	102.2 ± 0.510-24cm3	101.126	94.994	98.444	99.322	99.019
Exemestane	34.0 ± 0.5 10-24cm3	44.632	48.264	26.982	44.920	45.103
Fulvestrant	61.1 ± 0.5 10-24cm3	69.474	71.655	74.442	72.970	73.474
Ixabepilone	55.5 ± 0.5 10-24cm3	52.235	57.036	59.613	57.987	58.289
Letrozole	34.5 ± 0.5 10-24cm3	27.104	26.941	29.254	27.207	27.155
Megestrol Acetate	42.2 ± 0.5 10-24cm3	49.768	52.393	48.593	46.723	46.946
Methotrexate	47.2 ± 0.5 10-24cm3	36.250	32.866	36.632	35.136	34.928
Tamoxifen	47.1 ± 0.5 10-24cm3	39.929	36.784	39.793	38.689	38.330
Thiotepa	19.5 ± 0.5 10-24cm3	27.767	30.914	31.573	29.374	29.448

$$\begin{aligned}
 &+ [(8)^2 + (8)^2](1) + [(8)^2 + (9)^2](1) + [(8)^2 + (10)^2](1) \\
 &+ [(9)^2 + (9)^2](2) + [(9)^2 + (12)^2] \\
 &= 3428 \\
 &= [(3).(9)](1) + [(4).(7)](6) + [(4).(8)](2) + [(4).(9)](7) + [(4).(10)](2) \\
 &+ [(7).(9)](2) + [(8).(8)](1) + [(8).(9)](1) + [(8).(10)](1) \\
 &+ [(9).(9)](2) + [(9).(10)](1) + [(9).(12)](3) \\
 &= 1509
 \end{aligned}$$

2. By using Eq. (2) and edge partitions given in Table x we get,

$$\begin{aligned}
 M_2^*(G) &= \sum_{uv \in E(G)} [\eta_G(u) \cdot \eta_G(v)]. \\
 &= \sum_{uv \in E_1} [\eta_G(u) \cdot \eta_G(v)] + \sum_{uv \in E_2} [\eta_G(u) \cdot \eta_G(v)] + \sum_{uv \in E_3} [\eta_G(u) \cdot \eta_G(v)] \\
 &+ \sum_{uv \in E_4} [\eta_G(u) \cdot \eta_G(v)] + \sum_{uv \in E_5} [\eta_G(u) \cdot \eta_G(v)] + \sum_{uv \in E_6} [\eta_G(u) \cdot \eta_G(v)] \\
 &+ \sum_{uv \in E_7} [\eta_G(u) \cdot \eta_G(v)] + \sum_{uv \in E_8} [\eta_G(u) \cdot \eta_G(v)] + \sum_{uv \in E_9} [\eta_G(u) \cdot \eta_G(v)] \\
 &+ \sum_{uv \in E_{10}} [\eta_G(u) \cdot \eta_G(v)] + \sum_{uv \in E_{11}} [\eta_G(u) \cdot \eta_G(v)] + \sum_{uv \in E_{12}} [\eta_G(u) \cdot \eta_G(v)]
 \end{aligned}$$

3. By using Eq. (3) and the edge partitions given in Table X we get

$$\begin{aligned}
 HM_N(G) &= \sum_{uv \in E(G)} [\eta_G(u) + \eta_G(v)]^2. \\
 &= \sum_{uv \in E_1} [\eta_G(u) + \eta_G(v)]^2 + \sum_{uv \in E_2} [\eta_G(u) + \eta_G(v)]^2 + \sum_{uv \in E_3} [\eta_G(u) + \eta_G(v)]^2 \\
 &+ \sum_{uv \in E_4} [\eta_G(u) + \eta_G(v)]^2 + \sum_{uv \in E_5} [\eta_G(u) + \eta_G(v)]^2 + \sum_{uv \in E_6} [\eta_G(u) + \eta_G(v)]^2 \\
 &+ \sum_{uv \in E_7} [\eta_G(u) + \eta_G(v)]^2 + \sum_{uv \in E_8} [\eta_G(u) + \eta_G(v)]^2 + \sum_{uv \in E_9} [\eta_G(u) + \eta_G(v)]^2
 \end{aligned}$$

$$\begin{aligned}
 & + \sum_{uv \in E_{10}} [\eta_G(u) + \eta_G(v)]^2 + \sum_{uv \in E_{11}} [\eta_G(u) + \eta_G(v)]^2 + \sum_{uv \in E_{12}} [\eta_G(u) + \eta_G(v)]^2 \\
 & = [(3 + 9)^2](1) + [(4 + 7)^2](6) + [(4 + 8)^2](2) + [(4 + 9)^2](7) \\
 & + [(4 + 10)^2](2) + [(7 + 9)^2](2) + [(8 + 8)^2](1) + [(8 + 9)^2](1) \\
 & + [(8 + 10)^2](1) + [(9 + 9)^2](2) + [(9 + 10)^2](1) + [(9 + 12)^2](3) \\
 & = 6446
 \end{aligned}$$

4. By using Eq. (4) and vertex partitions given in table ix we get

$$\begin{aligned}
 M_N(G) &= \sum_{v \in V(G)} [\eta_G(v)]^2 \\
 &= \sum_{v \in V_1} [\eta_G(v)]^2 + \sum_{v \in V_2} [\eta_G(v)]^2 + \sum_{v \in V_3} [\eta_G(v)]^2 + \sum_{v \in V_4} [\eta_G(v)]^2 \\
 &+ \sum_{v \in V_5} [\eta_G(v)]^2 + \sum_{v \in V_6} [\eta_G(v)]^2 + \sum_{v \in V_7} [\eta_G(v)]^2 \\
 &= [(3)^2](1) + [(4)^2](17) + [(7)^2](2) + [(8)^2](2) + [(9)^2](5) + [(10)^2](1) \\
 &+ [(12)^2](1) \\
 &= 1156
 \end{aligned}$$

5. By using Eq. (5) and vertex partitions given in table ix we get

$$\begin{aligned}
 F_N(G) &= \sum_{v \in V(G)} [\eta_G(v)]^3 \\
 &= \sum_{v \in V_1} [\eta_G(v)]^3 + \sum_{v \in V_2} [\eta_G(v)]^3 + \sum_{v \in V_3} [\eta_G(v)]^3 + \sum_{v \in V_4} [\eta_G(v)]^3 \\
 &+ \sum_{v \in V_5} [\eta_G(v)]^3 + \sum_{v \in V_6} [\eta_G(v)]^3 + \sum_{v \in V_7} [\eta_G(v)]^3 \\
 &= [(3)^3](1) + [(4)^3](17) + [(7)^3](2) + [(8)^3](2) + [(9)^3](5) + [(10)^3](1) \\
 &+ [(12)^3](1) \\
 &= 9198
 \end{aligned}$$

Table ix
Vertex partition of Cyclophosphamide drug.

$\eta_v(G)$	Frequency
3	1
4	17
7	2
8	2
9	5
10	1
12	1

Table x

Edge partition of Cyclophosphamide drug.

(s, t)	Frequency
(3, 9)	1
(4, 7)	6
(4, 8)	2
(4, 9)	7
(4, 10)	2
(7, 9)	2
(8, 8)	1
(8, 9)	1
(8, 10)	1
(9, 9)	2
(9, 10)	1
(9, 12)	3

The topological indices of other drugs are obtained using similar computational techniques as those used in Theorems 1 - 5 above. The computed values of the topological indices for all 14 drugs are given in Table 1.

2.2. Quantitative structure-property relationship analysis

2.2.1. Regression models

Five topological indices are applied to model seven physical properties (boiling point (BP), melting point (MP), enthalpy of vaporization (E), flashpoint (F), molar refractivity (MR), molar volume (MV), and polarizability (P)) of the 14 anti-breast cancer drugs shown in Fig. 1. The experimental physical properties of these drugs are presented in Table 2 below. A simple linear regression model was used to correlate the computed values of topological indices with the experimental physical properties of drugs.

$$p = A + b[TI] \tag{6}$$

Here, A = constant, b = regression coefficient, TI = topological index, p = physical property.

For seven physical characteristics and five degree based topological indices of the molecular structure of fourteen medicines, constant (A) and regression coefficient (b) are computed using the SPSS tool. The following regression models are constructed for the specified degree based topological indices by using Eq. (6).

1. Regression model for modified neighborhood version of Forgotten topological index (F_N^*)

$$\text{Boiling Point} = 290.227 + 0.037[F_N^*(G)]$$

$$\text{Melting Point} = -79.851 + 0.0413[F_N^*(G)]$$

$$\text{Enthalpy} = 39.482 + 0.0033[F_N^*(G)]$$

$$\text{Flash Point} = 95.358 + 0.0243[F_N^*(G)]$$

$$\text{Molar Refraction} = 37.990 + 0.0108[F_N^*(G)]$$

$$\text{Molar Volume} = 65.428 + 0.0360[F_N^*(G)]$$

$$\text{Polarizability} = 15.047 + 0.0042[F_N^*(G)]$$

2. Regression model for neighborhood version of second Zagreb index

$$M_2^*(G)$$

$$\text{Boiling Point} = 257.017 + 0.0902[M_2^*(G)]$$

$$\text{Melting Point} = -123.529 + 0.1026[M_2^*(G)]$$

$$\text{Enthalpy} = 38.783 + 0.0144[M_2^*(G)]$$

$$\text{Flash Point} = 76.127 + 0.058[M_2^*(G)]$$

$$\text{Molar Refraction} = 28.842 + 0.026[M_2^*(G)]$$

$$\text{Molar Volume} = 33.042 + 0.0880[M_2^*(G)]$$

$$\text{Polarizability} = 11.420 + 0.0104[M_2^*(G)]$$

3. Regression model for Neighborhood version of Hyper Zagreb Index $HM_N(G)$.

$$\text{Boiling Point} = 261.120 + 0.0208[HM_N(G)]$$

$$\text{Melting Point} = -117.725 + 0.023[HM_N(G)]$$

$$\text{Enthalpy} = 41.739 + 0.0031[HM_N(G)]$$

$$\text{Flash Point} = 78.877 + 0.0134[HM_N(G)]$$

$$\text{Molar Refraction} = 30.172 + 0.0060[HM_N(G)]$$

$$\text{Molar Volume} = 36.142 + 0.0203[HM_N(G)]$$

$$\text{Polarizability} = 11.948 + 0.0023[HM_N(G)]$$

4. Regression model for Neighborhood Zagreb index $M_N(G)$.

$$\text{Boiling Point} = 249.20 + 0.123[M_N(G)]$$

$$\text{Melting Point} = -147.315 + 0.145[M_N(G)]$$

$$\text{Enthalpy} = 37.718 + 0.0197[M_N(G)]$$

$$\text{Flash Point} = 73.612 + 0.791[M_N(G)]$$

$$\text{Molar Refraction} = 25.462 + 0.0363[M_N(G)]$$

$$\text{Molar Volume} = 27.063 + 0.119[M_N(G)]$$

$$\text{Polarizability} = 10.080 + 0.014[M_N(G)]$$

5. Regression model for the neighborhood version of the Forgotten Topological index $F_N(G)$.

$$\text{Boiling Point} = 272.116 + 0.0131[F_N(G)]$$

$$\text{Melting Point} = -106.954 + 0.0150[F_N(G)]$$

$$\text{Enthalpy} = 40.969 + 0.002[F_N(G)]$$

$$\text{Flash Point} = 85.222 + 0.0085[FF_N(G)]$$

$$\text{Molar Refraction} = 34.803 + 0.0037[F_N(G)]$$

$$\text{Molar Volume} = 48.980 + 0.0128[F_N(G)]$$

$$\text{Polarizability} = 13.785 + 0.0015[F_N(G)]$$

Table 3 lists the correlation coefficients for each topological index and the seven physical properties. Fig. 2 depicts the relationship between the drug's topological index and the correlation coefficient of its physicochemical attributes like boiling point, melting point, enthalpy, flashpoint, molar refraction, molar volume, and polarizability.

2.2.2. Evaluation of statistical parameters

This section uses QSPR modeling to analyze the correlation between

the physicochemical features of various breast cancer drugs such as Abemaciclib (Verzenio), Abraxane, Anastrozole (Arimidex), Capecitabine (Xeloda), Cyclophosphamide, Everolimus (Afinitor), Exemestane (Aromasin), Fulvestrant (Faslodex), Ixabepilone (Ixempra), Letrozole (Femara), Megestrol Acetate, Methotrexate, Tamoxifen (Soltamox), and Thiotepa (Tepadina), and their computed degree based TIs. Such as N is a sample size, A is Y -intercept or constant, b is slope, r is the correlation coefficient, r^2 is the ratio of the dependent variable change that a linear regression model explains. We believe the correlation coefficient to be one where the theoretical and experimental calculations are closer (indicated by bolded font in tables). This form of test can help relate and determine model improvement. It must be noted that the value of p is less than 0.05 and the value of r is even more than 0.6. Consequently, it depicts that all the properties are significant. The statistical variables involved in QSPR models of TIs are presented in Tables 4–8. The term “standard error estimate” refers to the amount of variance for an observation observed around the determined regression line. It is described in Table 9 and assesses the degree of prediction accuracy produced around the calculated regression line.

2.2.3. Comparison

In this section, the evaluation of experimental values and calculated values from our regression models are performed. The physical characteristics of the practical and theoretically computed values of the models are also compared, and the results are presented in Tables 10–16.

The detailed QSPR analysis results show that, as per the horizontal analysis of correlation coefficients for the physical properties, the neighborhood Zagreb index provides the highest correlation coefficient for molar refraction and polarizability as $r = 0.953$. Additionally, it exhibits a high correlation of $r = 0.90$ with boiling point. The neighborhood version of the Forgotten Topological index gives a maximum correlation for molar volume that is $r = 0.941$. Modified Neighborhood Version of the Forgotten Topological index ($FN^*(G)$) and Neighborhood Version of the Second Zagreb Index ($M2^*(G)$, along with $HM_N(G)$) yields a substantial correlation coefficient of $r = 0.95$ with molar volume. These results confirmed the potential of the considered topological indices as a tool for drug discovery and design in the field of breast cancer treatment. This work showed how the topological indices calculated in this article could contribute to the design of new pharmaceuticals by chemists and other individuals working in the pharmaceutical sector. Different formulations of these medications may be utilized to treat various disorders; this would depend on the range of TIs that were calculated for this work.

3. Conclusion

In this article, a Quantitative Structure Property Relationship (QSPR) analysis is carried out using some novel degree-based topological indices and regression models to predict various physical properties (such as boiling point, melting point, enthalpy, flash point, molar refraction, molar volume, and polarizability) of 14 drugs used for the breast cancer treatment. The molecular structures of these drugs are topologically modeled through vertex and edge partitioning techniques of graph theory, and then a linear regression model is developed to correlate the computed values with the experimental properties of the drugs to investigate the performance of TIs in predicting these properties. The detailed QSPR analysis results show that, as per the horizontal analysis of correlation coefficients for the physical properties, the neighborhood Zagreb index provides the highest correlation coefficient for molar refraction and polarizability as $r = 0.953$. Additionally, it exhibits a high correlation of $r = 0.90$ with boiling point. The neighborhood version of the Forgotten Topological index gives a maximum correlation for molar volume, that is $r = 0.941$. Modified Neighborhood Version of the Forgotten Topological index ($FN^*(G)$) and Neighborhood Version of the Second Zagreb Index ($M2^*(G)$, along with $HM_N(G)$) yields a sub-

stantial correlation coefficient of $r = 0.95$ with molar volume. These results confirmed the potential of the considered topological indices as a tool for drug discovery and design in the field of breast cancer treatment. This work showed how the topological indices calculated in this article could contribute to the design of new pharmaceuticals by chemists and other individuals working in the pharmaceutical sector. Different formulations of these medications may be utilized to treat various disorders; this would depend on the range of TIs that were calculated for this work. It will be simple for the analyst to create new pharmaceuticals based on the combinations of positively maximum correlated drugs, now that we have constituted the correlation coefficient for various topological indices. The relationship concerning topological indices and the physical properties of multiple drugs used in the cure or prevention of a specific disease can be constructed like this.

Ethical approval

Not applicable.

Funding

The authors Asad Ullah, Summeira Meharban, and Anila Humraz gratefully acknowledge the financial support from the Higher Education Commission of Pakistan (Grant No. 20-11682/NRPU/R&D/HEC/2020) to conduct this study.

Availability of data and materials

All data generated or analyzed during this study are included in this article.

CRediT authorship contribution statement

Summeira Meharban: Conceptualization, Methodology, Software, Formal analysis, Investigation, Validation, Data curation, Visualization, Writing – original draft. **Asad Ullah:** Conceptualization, Methodology, Formal analysis, Validation, Writing – original draft, Writing – review & editing, Supervision, Project administration, Resources, Funding acquisition. **Shahid Zaman:** Conceptualization, Methodology, Formal analysis, Writing – review & editing. **Anila Hamraz:** Methodology, Software, Validation. **Abdul Razaq:** Validation, Writing – review & editing.

Declaration of competing interest

The authors declare that they have no known competing financial interests or personal relationships that could have appeared to influence the work reported in this paper.

Data availability

All data generated or analyzed during this study are included in this article.

References

- Ali, P., Kirmani, S.A.K., Al Rugaie, O., Azam, F., 2020. Degree-based topological indices and polynomials of hyaluronic acid-curcumin conjugates. *Saudi Pharmaceut. J.* 28 (9), 1093–1100. <https://doi.org/10.1016/j.jsps.2020.07.010>.
- Arockiaraj, M., Klavzar, S., Clement, J., Mushtaq, S., Balasubramanian, K., 2019. Edge distance-based topological indices of strength-weighted graphs and their application to coronoid systems, carbon nanocones and SiO(2) nanostructures. *Mol Inform* 38 (11–12), e1900039. <https://doi.org/10.1002/minf.201900039>.
- Arockiaraj, M., Paul, D., Clement, J., Tigga, S., Jacob, K., Balasubramanian, K., 2023. Novel molecular hybrid geometric-harmonic-Zagreb degree based descriptors and their efficacy in QSPR studies of polycyclic aromatic hydrocarbons. *SAR QSAR Environ. Res.* 34 (7), 569–589. <https://doi.org/10.1080/1062936X.2023.2239149>.
- Aslam, A., Ahmad, S., Gao, W., 2017a. On certain topological indices of boron triangular nanotubes. *Z. Naturforsch.* 72 (8), 711–716.

- Aslam, A., Bashir, Y., Ahmad, S., Gao, W., 2017b. On topological indices of certain dendrimer structures. *Z. Naturforsch.* 72 (6), 559–566.
- Bokhary, S.A.U.H., Adnan, Siddiqui, M.K., Cancan, M., 2021. On topological indices and QSPR analysis of drugs used for the treatment of breast cancer. *Polycycl. Aromat. Comp.* 42 (9), 6233–6253. <https://doi.org/10.1080/10406638.2021.1977353>.
- Duchowicz, P.R., Talevi, A., Bruno-Blanch, L.E., Castro, E.A., 2008. New QSPR study for the prediction of aqueous solubility of drug-like compounds. *Bioorg. Med. Chem.* 16 (17), 7944–7955.
- Figuerola, B., Avila, C., 2019. The phylum bryozoa as a promising source of anticancer drugs. *Mar. Drugs* 17 (8). <https://doi.org/10.3390/md17080477>.
- Furtula, B., Gutman, I., 2015. A forgotten topological index. *J. Math. Chem.* 53 (4), 1184–1190. <https://doi.org/10.1007/s10910-015-0480-z>.
- Furtula, B., Gutman, I., Dehmer, M., 2013. On structure-sensitivity of degree-based topological indices. *Appl. Math. Comput.* 219 (17), 8973–8978. <https://doi.org/10.1016/j.amc.2013.03.072>.
- Gao, W., Wang, W., Farahani, M.R., 2016a. Topological indices study of molecular structure in anticancer drugs. *J. Chem.*, 3216327 <https://doi.org/10.1155/2016/3216327>, 2016.
- Gao, W., Wang, W., Farahani, M.R., 2016b. Topological indices study of molecular structure in anticancer drugs. *J. Chem.* 1–8. <https://doi.org/10.1155/2016/3216327>, 2016.
- Gutman, I., Furtula, B., Katanić, V., 2018. Randić index and information. *AKCE International Journal of Graphs and Combinatorics* 15 (3), 307–312.
- Gutman, I., Trinajstić, N., 1972. Graph theory and molecular orbitals. Total ϕ -electron energy of alternant hydrocarbons. *Chem. Phys. Lett.* 17 (4), 535–538. [https://doi.org/10.1016/0009-2614\(72\)85099-1](https://doi.org/10.1016/0009-2614(72)85099-1).
- Hakeem, A., Ullah, A., Zaman, S., 2023. Computation of some important degree-based topological indices for γ -graphyne and Zigzag graphyne nanoribbon. *Mol. Phys.*, e2211403 <https://doi.org/10.1080/00268976.2023.2211403>.
- Hayat, S., Khan, M.A., Khan, A., Jamil, H., Malik, M.Y.H., 2023a. Extremal hyper-Zagreb index of trees of given segments with applications to regression modeling in QSPR studies. *Alex. Eng. J.* 80, 259–268. <https://doi.org/10.1016/j.aej.2023.08.051>.
- Hayat, S., Khan, S., Khan, A., Liu, J.-B., 2022. Valency-based molecular descriptors for measuring the π -electronic energy of lower polycyclic aromatic hydrocarbons. *Polycycl. Aromat. Comp.* 42 (4), 1113–1129. <https://doi.org/10.1080/10406638.2020.1768414>.
- Hayat, S., Suhaili, N., Jamil, H., 2023b. Statistical significance of valency-based topological descriptors for correlating thermodynamic properties of benzenoid hydrocarbons with applications. *Computational and Theoretical Chemistry* 1227, 114259. <https://doi.org/10.1016/j.comptc.2023.114259>.
- Hosamani, S., Perigidad, D., Jamagoud, S., Maled, Y., Gavade, S., 2017. QSPR analysis of certain degree based topological indices. *Journal of Statistics Applications & Probability* 6 (2), 361–371.
- Jahanbani, A., Shao, Z., Sheikholeslami, S.M., 2021. Calculating degree based multiplicative topological indices of Hyaluronic Acid-Paclitaxel conjugates' molecular structure in cancer treatment. *J. Biomol. Struct. Dyn.* 39 (14), 5304–5313. <https://doi.org/10.1080/07391102.2020.1800512>.
- Janoschek, R., 1987, 1986. 28 Abb., X, 212 S., DM 128,-. ISBN 3-540-16235-6. *Nachrichten aus Chemie, Technik und Laboratorium*. In: Gutman und, Von I., Polansky, O.E. (Eds.), *Mathematik und Konstitutionsformeln: Mathematical Concepts in Organic Chemistry*, vol. 35. Springer-Verlag, Berlin - Heidelberg - New York - Tokyo, pp. 34–41. <https://doi.org/10.1002/nadc.19870350115>, 1.
- Joudaki, D., Shafiei, F., 2020. QSPR models to predict thermodynamic properties of cycloalkanes using molecular descriptors and GA-MLR method. *Curr. Comput. Aided Drug Des.* 16 (1), 6–16.
- Kinteh, B., Kinteh, S.L.S., Jammeh, A., Touray, E., Barrow, A., 2023. Breast cancer screening: knowledge, attitudes, and practices among female university students in the Gambia. *BioMed Res. Int.* 2023, 9239431 <https://doi.org/10.1155/2023/9239431>.
- Kumar, S., Ahmad, M.K., Waseem, M., Pandey, A.K., 2015. Drug targets for cancer treatment: an overview. *Med chem* 5 (3), 115–123.
- Kwon, Y.C., Ali, A., Nazeer, W., Ahmad Chaudhary, M., Kang, S.M., 2018. M-polynomials and degree-based topological indices of triangular, hourglass, and jagged-rectangle benzenoid systems. *J. Chem.*, 8213950 <https://doi.org/10.1155/2018/8213950>, 2018.
- Liu, J.-B., Iqbal, H., Shahzad, K., 2022. Topological properties of concealed non-kekulean benzenoid hydrocarbon. *Polycycl. Aromat. Comp.* 43 (2), 1776–1787. <https://doi.org/10.1080/10406638.2022.2039230>.
- Mc, S., B, N.S., A, K.N., 2020. Predicting physico-chemical properties of octane isomers using QSPR approach. *Malaya J. Matematik* 8, 104–116. <https://doi.org/10.26637/MJM0801/0018>.
- Mondal, S., De, N., Pal, A., 2019. On some new neighbourhood degree based indices. *Acta Chem. Iasi* 27 (1), 31–46. <https://doi.org/10.2478/achi-2019-0003>.
- Mondal, S., De, N., Pal, A., Gao, W., 2021. Molecular descriptors of some chemicals that prevent COVID-19. *Curr. Org. Synth.* 18 (8), 729–741. <https://doi.org/10.2174/1570179417666201208114509>.
- Muhammad, U., Uzairu, A., Ebuka Arthur, D., 2018. Review on: Quantitative structure activity relationship (QSAR) modeling. *J. Anal. Pharm. Res* 7 (2), 240.
- Nantasenamat, C., Isarankura-Na-Ayudhya, C., Naenna, T., Prachayasittikul, V., 2009. A Practical Overview of Quantitative Structure-Activity Relationship.
- Nantasenamat, C., Isarankura-Na-Ayudhya, C., Prachayasittikul, V., 2010. Advances in computational methods to predict the biological activity of compounds. *Expet Opin. Drug Discov* 5 (7), 633–654. <https://doi.org/10.1517/17460441.2010.492827>.
- Paul, D., Arockiaraj, M., Jacob, K., Clement, J., 2023. Multiplicative versus scalar multiplicative degree based descriptors in QSAR/QSPR studies and their

- comparative analysis in entropy measures. *The European Physical Journal Plus* 138 (4), 323. <https://doi.org/10.1140/epjp/s13360-023-03920-7>.
- Randic, M., 1996. Quantitative structure-property relationship. Boiling points of planar benzenoids. *New J. Chem.* 20, 1001–1009.
- Rauf, A., Naeem, M., Rahman, J., Saleem, A.V., 2022. QSPR study of ve-degree based end vertice edge entropy indices with physio-chemical properties of breast cancer drugs. *Polycycl. Aromat. Comp.* 1–14. <https://doi.org/10.1080/10406638.2022.2086272>.
- Shanmukha, M., Usha, A., Praveen, B., Douhadji, A., 2022. Degree-based molecular descriptors and QSPR analysis of breast cancer drugs. *J. Math.* 2022, 1–13.
- Shanmukha, M.C., Usha, A., Praveen, B.M., Douhadji, A., 2022. Degree-based molecular descriptors and QSPR analysis of breast cancer drugs. *J. Math.* 2022, 5880011 <https://doi.org/10.1155/2022/5880011>.
- Shao, Z., Siddiqui, M.K., Muhammad, M.H., 2018. Computing Zagreb indices and Zagreb polynomials for symmetrical nanotubes. *Symmetry* 10 (7), 244.
- Shirdel, G., Rezapour, H., Sayadi, A., 2013. The Hyper-Zagreb Index of Graph Operations.
- Siddiqui, M.K., Imran, M., Ahmad, A., 2016. On Zagreb indices, Zagreb polynomials of some nanostar dendrimers. *Appl. Math. Comput.* 280, 132–139.
- Siddiqui, M.K., Javed, S., Khalid, S., Amin, N., Hussain, M., 2022. On network construction and module detection for molecular graph of titanium dioxide. *J. Biomol. Struct. Dyn.* 1–13. <https://doi.org/10.1080/07391102.2022.2155703>.
- Todeschini, R., Consonni, V., 2009. *Molecular Descriptors for Chemoinformatics*.
- Ullah, A., Bano, Z., Zaman, S., 2023a. Computational aspects of two important biochemical networks with respect to some novel molecular descriptors. *J. Biomol. Struct. Dyn.* 1–15. <https://doi.org/10.1080/07391102.2023.2195944>.
- Ullah, A., Jabeen, S., Zaman, S., Hamraz, A., Meherban, S., 2024. Predictive potential of K-Banhatti and Zagreb type molecular descriptors in structure–property relationship analysis of some novel drug molecules. *J. Chin. Chem. Soc.* <https://doi.org/10.1002/jccs.202300450>. $n/a(n/a)$.
- Ullah, A., Qasim, M., Zaman, S., Khan, A., 2022a. Computational and comparative aspects of two carbon nanosheets with respect to some novel topological indices. *Ain Shams Eng. J.* 13 (4), 101672 <https://doi.org/10.1016/j.asej.2021.101672>.
- Ullah, A., Shamsudin, Zaman, S., Hamraz, A., 2023b. Zagreb connection topological descriptors and structural property of the triangular chain structures. *Phys. Scripta* 98 (2), 025009. <https://doi.org/10.1088/1402-4896/acb327>.
- Ullah, A., Shamsudin, Zaman, S., Hamraz, A., Saeedi, G., Caceres, J.O., 2022b. Network-based modeling of the molecular topology of fuchsine acid dye with respect to some irregular molecular descriptors. *J. Chem.* 2022, 1–8. <https://doi.org/10.1155/2022/8131276>.
- Ullah, A., Zeb, A., Zaman, S., 2022c. A new perspective on the modeling and topological characterization of H-Naphtalenic nanosheets with applications. *J. Mol. Model.* 28 (8), 211. <https://doi.org/10.1007/s00894-022-05201-z>.
- Varmuza, K., Filzmoser, P., Dehmer, M., 2013. Multivariate linear QSPR/QSAR models: rigorous evaluation of variable selection for PLS. *Comput. Struct. Biotechnol. J.* 5 (6), e201302007.
- Waks, A.G., Winer, E.P., 2019. Breast cancer treatment: a review. *JAMA* 321 (3), 288–300. <https://doi.org/10.1001/jama.2018.19323>.
- Wiener, H., 1947. Structural determination of paraffin boiling points. *J. Am. Chem. Soc.* 69 (1), 17–20. <https://doi.org/10.1021/ja01193a005>.
- Xu, H.-Y., Zou, J.-W., Yu, Q.-S., Wang, Y.-H., Zhang, J.-Y., Jin, H.-X., 2007. QSPR/QSAR models for prediction of the physicochemical properties and biological activity of polybrominated diphenyl ethers. *Chemosphere* 66, 1998–2010. <https://doi.org/10.1016/j.chemosphere.2006.07.072>.
- Yan, T., Kosar, Z., Aslam, A., Zaman, S., Ullah, A., 2023. Spectral techniques and mathematical aspects of K4 chain graph. *Phys. Scripta* 98 (4), 045222. <https://doi.org/10.1088/1402-4896/acc4f0>.
- Yu, X., Zaman, S., Ullah, A., Saeedi, G., Zhang, X., 2023. Matrix analysis of hexagonal model and its applications in global mean-first-passage time of random walks. *IEEE Access* 11, 10045–10052. <https://doi.org/10.1109/access.2023.3240468>.
- Zaman, S., Jalani, M., Ullah, A., Ahmad, W., Saeedi, G., 2023a. Mathematical analysis and molecular descriptors of two novel metal–organic models with chemical applications. *Sci. Rep.* 13 (1), 5314. <https://doi.org/10.1038/s41598-023-32347-4>.
- Zaman, S., Jalani, M., Ullah, A., Ali, M., Shahzadi, T., 2023b. On the topological descriptors and structural analysis of cerium oxide nanostructures. *Chem. Pap.* 77 (5), 2917–2922. <https://doi.org/10.1007/s11696-023-02675-w>.
- Zaman, S., Jalani, M., Ullah, A., Saeedi, G., Guardo, E., 2022. Structural analysis and topological characterization of sudoku nanosheet. *J. Math.* 2022, 1–10. <https://doi.org/10.1155/2022/5915740>.
- Zaman, S., Ullah, A., 2023. Kemeny's constant and global mean first passage time of random walks on octagonal cell network. <https://doi.org/10.1002/mma.9046>. *Mathematical Methods in the Applied Sciences*, $n/a(n/a)$.
- Zhang, X., Aslam, A., Saeed, S., Razzaque, A., Kanwal, S., 2023. Investigation for metallic crystals through chemical invariants, QSPR and fuzzy-TOPSIS. *J. Biomol. Struct. Dyn.* 1–12. <https://doi.org/10.1080/07391102.2023.2209656>.
- Zhong, J.-F., Rauf, A., Naeem, M., Rahman, J., Aslam, A., 2021. Quantitative structure-property relationships (QSPR) of valency based topological indices with Covid-19 drugs and application. *J. Arabian Journal of Chemistry* 14 (7), 103240.